MCB Accepts, published online ahead of print on 13 November 2006
Mol. Cell. Biol. doi:10.1128/MCB.00461-06

The PH domain proteins Slm1 and Slm2 are targets of sphingolipid signaling during the response to heat stress

Alexes Daquinag[$,1], Maria Fadri[$,1], Sung Yun Jung[#], Jun Qin[#], and Jeannette Kunz[$]*

[$]Department of Molecular Physiology and Biophysics
and [#]Department of Biochemistry and Molecular Biology
Baylor College of Medicine,
Houston, Texas 77030

Running title: Slm phosphorylation is required for survival under heat stress

Word count: Introduction, Results, Discussion: **7903**
Methods and Materials: **1998**

*To whom correspondence should be addressed:
Jeannette Kunz
Department of Molecular Physiology & Biophysics
Baylor College of Medicine
One Baylor Plaza, BCM335, RM T419
Houston, TX 77030
Email: jkunz@bcm.tmc.edu
Tel.: 713-798 5797
Fax: 713-798 3475

1 These two authors contributed equally to this work

-

ABSTRACT

The PH domain containing proteins Slm1 and Slm2 were previously identified as effectors of the PI4,5P_2 and TORC2 signaling pathways. Here, we demonstrate that Slm1 and Slm2 are also targets of sphingolipid signaling during the heat shock response. We show that upon depletion of cellular sphingolipid levels, Slm1 function becomes essential for survival under heat stress. We further demonstrate that Slm proteins are regulated by a phosphorylation/dephosphorylation cycle involving the sphingolipid-activated protein kinases Pkh1/Pkh2 and the calcium/calmodulin-dependent protein phosphatase calcineurin. By using a combination of mass spectrometry and mutational analysis, we identify serine residue 659 in Slm1 as a site of phosphorylation. Characterization of Slm1 mutants that mimic dephosphorylated and phosphorylated states, respectively, demonstrates that phosphorylation at serine 659 is vital for survival under heat stress and promotes the proper polarization of the actin cytoskeleton. Finally, we present evidence that Slm proteins are also required for the trafficking of the raft-associated arginine permease Can1 to the plasma membrane, a process that requires sphingolipid synthesis and actin polymerization. Together with previous work, our findings suggest that Slm proteins are subject to regulation by multiple signals, including PI4,5P_2, TORC2, and sphingolipids, and may thus integrate inputs from different signaling pathways to temporally and spatially control actin polarization.

INTRODUCTION

Sphingolipids have emerged as key regulators of diverse cellular processes in eukaryotic cells (17, 18). Sphingolipids are major components of eukaryotic cell membranes, particularly the plasma membrane where they serve important structural roles. More recently, it has been realized that sphingolipids also play vital regulatory roles. Studies in both mammalian cells and yeast have shown that sphingolipids, together with ergosterol (or cholesterol in mammalian cells), have the tendency to cluster together and form membrane microdomains or lipid rafts, which are thought to act as platforms for the organization and regulation of signal transduction cascades and membrane trafficking events(50).

Specifically, in the yeast *Saccharomyces cerevisiae*, sphingolipids mediate diverse cellular functions required for cell growth, calcium homeostasis, actin cytoskeletal organization, endocytosis and secretion, and the cellular response to environmental stress (17, 18, 24). In yeast, signaling roles for sphingolipids have been well established during the response to heat stress conditions (10, 11). The *de novo* synthesis of sphingolipids is transiently induced in response to heat shock causing a 2-100 fold increased in the sphingoid bases phytosphingosine (PHS) and dihydrosphingosine (DHS) and accumulation of their metabolites (19, 32, 58). PHS and DHS were shown to act as signaling molecules and to directly activate a pair of functionally redundant protein kinases termed Pkh1 and Pkh2, the yeast homologs of mammalian phosphoinositide-dependent protein kinase-1 (9, 22). Pkh1 and Pkh2, in turn, phosphorylate and activate downstream protein kinases including Pkc1, Sch9 and the related Ypk1 and Ypk2 (9, 29, 46, 47). Together, these kinases are thought to mediate sphingolipid-dependent signaling under

heat stress and non-stress conditions. However, little is known about the targets of sphingolipid dependent signaling or how those targets regulate the cellular machinery.

In addition to inducing an increase in *de novo* sphingolipid synthesis, heat stress also stimulates a transient increase in the synthesis of the lipid second messenger phosphatidylinositol-4, 5-bisphosphate ($PI4,5P_2$) (16). $PI4,5P_2$ is a critical regulator of growth, actin cytoskeletal dynamics, and a variety of other cellular processes (55, 59). Interestingly, yeast mutants lacking $PI4,5P_2$ synthesis exhibit many of the same phenotypes as mutants lacking sphingolipid biosynthesis or Pkh1/2 function, including the depolarization of the actin cytoskeleton, and defects in cell wall integrity and endocytosis (1, 15, 16, 28). These findings suggested the possibility of cross-talk between the two signaling pathways, and recent studies support a functional connection between $PI4,5P_2$ and sphingolipid signaling pathways. Specifically, deletion of *CSG2*, encoding the catalytic subunit of the enzyme that synthesizes the sphingolipid mannosylated-inositol-phosphoceramide (MIPC) leads to intracellular accumulation of the complex sphingolipid inositol-phosphoceramide (IPC) and thereby causes calcium sensitivity (6, 56). Isolation and identification of yeast mutants that suppress the calcium sensitive growth of the *csg2*Δ mutant subsequently identified genes involved in sphingolipid biosynthesis or signaling (5, 6, 61). In addition, these screens also identified a mutant in *MSS4*, the gene encoding the single essential PI4P 5-kinase that synthesizes $PI4,5P_2$ (Beeler et al, JBC 1998). These data thus imply a connection between sphingolipid and $PI4,5P_2$ signaling pathways, but the molecular mechanisms of how this might be achieved and the point(s) of convergence between the two pathways remained elusive.

One possible way of how sphingolipids may intersect with the $PI4,5P_2$ signaling pathway is to modulate the activation or localization of targets of $PI4,5P_2$ dependent signaling. The recently

identified redundant PI4,5P_2 effectors, Slm1 and Slm2, are essential for growth and actin cytoskeletal organization and require their PH domains for targeting to the plasma membrane in a PI4,5P_2–dependent manner (3, 20). Because Slm1 and Slm2 co-localize with the lipid raft-associated protein Pma1 (20), Slm1 and Slm2 are good candidates for linking sphingolipid and PI4,5P_2 signaling pathways. Furthermore, Slm1 and Slm2 also interact with and are regulated by the TORC2 signaling complex (3, 20) that controls growth and actin cytoskeleton organization in response to a variety of stress conditions including heat, cell wall and nutrient stress. *SLM1* was also isolated genetically as a dosage suppressor of the TORC2 component Avo3 (27). Interestingly, TORC2 components, including *TOR2* and *AVO3,* were identified among the collection of mutants that suppress the calcium-sensitive growth of the *csg2*Δ mutant (5, 6, 61) suggesting a functional link between Slms, TORC2 and sphingolipid metabolism. Taken together, these findings raise the possibility that Slm1 and Slm2 may be a point of convergence between sphingolipid, phosphoinositide and TORC2 signaling pathways and suggest that modulation of Slm function in response to environmental signals could be an efficient way of modulating the output of essential pathways to coordinate the cellular response to various stress conditions.

In the current study, we show that Slm proteins and sphingolipids cooperate to promote cell survival by regulating cell growth and proper actin polarization. We demonstrate that Slm phosphorylation during heat stress conditions is dependent on the activity of the sphingolipid-regulated protein kinases Pkh1 and Pkh2. Phosphorylation of Slm is antagonized by the Ca^{2+}/calmodulin dependent protein phosphatase calcineurin, which binds Slm1 and Slm2 via a conserved calcineurin-binding motif present in their C-termini. Genetic evidence places Slm1 in a branch of the Pkh1 and Pkh2 pathway and suggests that Slm proteins provide a subset of Pkh-

dependent functions required for proper actin polarization. Furthermore, Slm proteins and Pkh kinases are required for the trafficking of the raft-associated arginine permease Can1 to the plasma membrane, a process that is dependent on *de novo* sphingolipid biosynthesis and polymerized actin. Together with results obtained in previous studies, our data suggest that Slm1 and Slm2 link inputs from multiple signaling pathways to regulate actin polarization in response to various environmental stimuli.

MATERIALS AND METHODS

Materials, strains, and plasmids

Protease inhibitor mix lacking EDTA was obtained from Roche Immunochemicals. G418 and Pfx polymerase were from Invitrogen. Primestar Polymerase was from Takara Mirus Bio. (Madison, WI). GSH-conjugated agarose beads were from Clontech, IgG-conjugated sepharose beads were from Sigma-Aldrich, and mouse monoclonal anti-HA IgG conjugated to sepharose beads was from Babco. Mouse monoclonal anti-GST antibodies were from Sigma-Aldrich, mouse monoclonal anti-HA antibodies were from Babco, mouse monoclonal anti-TAP antibodies were from OpenBiosystems, Cy2-conjugated goat anti-mouse IgG and Cy3-conjugated goat anti-rabbit IgG were from Jackson ImmunoResearch, and Alexa-594-conjugated phalloidin was from Molecular Probes. Molecular mass standards were from Bio-Rad Laboratories. Myriocin and phytosphingosine were purchased from Sigma (St. Louis, MO). Myriocin was dissolved in ethanol at a stock concentration of 2mg/mL and was stored at 4˚C, whereas phytosphingosine was dissolved in ethanol at 15 mM and stored at –20˚C. FK506 was obtained from AG Scientific (San Diego, CA) and was dissolved in 90% ethanol/ 10% Tween-20 at a stock concentration of 10 mg/ml and stored at –20˚C. Anti-phosphoserine (Q5) and anti-phosphothreonine (Q7) antibodies were purchased from Qiagen (Hilden, Germany).

S. cerevisiae strains used are listed in Table I. Yeast strains from the yeast deletion collection were purchased from OpenBiosystems and backcrossed twice into the W303 strain background. Plasmids YCpG22-PKH1 (*GAL1*p-*PKH1 TRP1),* pJK702 (*GAL1*p-HA_2-*SLM1* in pAS25 YCplac33, *CEN, URA3*), and pJK708 (*6HIS-SLM2* in pET28a) have been previously described (18, 28). Plasmids pJK714 (*GST-*$SLM1_{\Delta CNA}$ in pEGKT or pAS25) and pJK715 (*GST-*$SLM2_{\Delta CNA}$ in pEGKT) containing Slm1 and Slm2 deletion mutants lacking the calcineurin

binding site were constructed as follows by PCR amplification using the following primer combinations: Slm1-CN-For: 5'-CTACTACTCGAGTTATTCATCATTTTCTACCATTGTGC; Slm1-CN-Rev: 5'- CTACTACTCGAGTTATTGATCTTGTAATTCAGAATCAT and Slm2-CN-For: 5'- CTACTACTCGAGTTACGTATGTTGCTCATTAGTTACC; Slm2-CN-Rev: 5-CTACTACTCGAGTTAATTCTGAATTTGTGAATCATTCG. Ser569 in Slm1 was mutagenized using the following primer combinations: Slm1S659A-For: 5'-ACATCCATGTCT**G**CATTACCTGATACT and Slm1S659A-Rev: 5'-AGTATCAGGTAATG**C**AGACATGGATGT; Slm1S659D-For: 5'-ACATCCATGTCT**GAC**TTACCTGATACT and Slm1S659D-Rev: 5'-AGTATCAGGTAA**GTC**AGACATGGTTGT. Bold, underlined residues indicate nucleotide changes in the mutants. All PCR products were digested with *XhoI* (site contained within primer sequences) and cloned into the *SalI* site in vector pEG-KT resulting in in-frame fusion with GST, into the *SalI* site of pAS25 resulting in in-frame fusion with HA, or into the *XhoI* site of vector p425GPD. DNA sequences were confirmed by sequencing.

General Genetic Manipulations

Wild type yeast strains and temperature-sensitive mutants were grown at 26˚C unless otherwise indicated. Media are described elsewhere (49). Unless otherwise indicated, YPD and SD medium contained 2% glucose, whereas YPG and SG medium contained 2% galactose, 2% raffinose as the carbon source. Strain construction followed standard methods (49). Yeast cells were transformed by the lithium acetate procedure (30) and transformants were selected on SD medium lacking the appropriate amino acid supplement for maintenance of the plasmid marker.

Quantitation of myriocin and canavanine sensitivity

Myriocin and PHS were stored as stock solutions at –20˚C and were prewarmed to room temperature before being added to media at the desired concentration. Canavanine (10 mg/ml in water) was stored at 4˚C. Sensitivity of the indicated yeast strains to drugs was tested by spotting serial dilutions (1:10) of yeast strains adjusted to A_{600} of 1.0 on YPD plates supplemented with various concentrations of myriocin, PHS or drug vehicle alone. For canavanine sensitivity, cultures were spotted on plates lacking arginine but containing canavanine (0.5 or 1 μg/ml). Plates were incubated at the indicated temperature for 3-4 days before photography.

Genetic interaction between *slm1*Δ and mutants in the sphingolipid biosynthetic pathway

Doubly heterozygous diploids were generated by crossing haploid strains and selecting for the presence of appropriate markers. To obtain double mutants the *slm1::KanMX* deletion strain in the W303 genetic background was mated with isogenic strains containing deletions in genes coding for enzymes in the sphingolipid biosynthesis pathway (Figure 1). Diploids were sporulated at 26°C, and tetrads were dissected and allowed to germinate at 26°C on YEPD medium and scored for G418 resistance or the presence of auxotrophic markers. Only tetrads that yielded four viable progeny of which two were G418 resistant and two were G418 sensitive were analyzed, with G418 resistant segregants being assumed to be double mutants. To test for synthetic sickness, growth of wild type, isogenic single and double mutant segregants was assayed by diluting overnight cultures to an A_{600} of 1.0 and spotting serial tenfold dilutions of the indicated strains onto YPD plates. Plates were incubated at 26˚C or 38° and growth was scored after 3 to 4 days.

Detection of Slm phosphorylation by immunoprecipitation and Western blotting

Slm phosphorylation was generally assayed in strains containing chromosomally expressed Slm1-TAP and Slm2-TAP under control of their endogenous promoter. Slm1-TAP was functional, because a yeast strain containing *SLM1-TAP* in combination with a deletion in *SLM2* was viable and grew like the wild type strain (data not shown). Cultures were grown in YPD medium at 26˚C to A_{600} of 1.0 and were then treated with vehicle alone, chemical inhibitors (myriocin, 2µg/ml; FK506, 2µg/ml; BAPTA, 10 mM) or other compounds (PHS, 10µM; $CaCl_2$, 100 mM) for additional 45 min. For heat shock experiments, cultures were then divided into aliquots and incubated shaking at either 26˚C or 38˚C for the indicated periods of times. To prepare whole cell extracts, yeast cells were collected by centrifugation for 4 min at 3000 x rpm at 4˚C, resuspended in lysis buffer (50 mM Tris-HCl pH 7.5, 50 mM NaCl, 0.1 mM EDTA, 0.1% NP-40, 10% glycerol, supplemented with complete protease inhibitor mix and 2 mM each of the phosphatase inhibitors NaF, $NaVO_3$, and β-glycerophosphate), lysed with glassbeads in a bead-beater (6 x 30 sec, 4°C, BioSpecs), and clarified by microcentrifugation (500 x g, 15 min at 4 °C). TAP-tagged Slm proteins were purified as described (25) from 5 mg whole cell extract (diluted 1:5 with lysis buffer), using an IgG-sepharose column followed by three washing steps with ice-cold lysis buffer. Bead-bound immune complexes were solubilized in SDS-PAGE sample buffer and immediately boiled for 5 min in a water bath and then clarified by brief centrifugation in a microcentrifuge before resolution by SDS-PAGE.

To compare Slm phosphorylation in wild type and *pkh1ts pkh2*Δ*, ypk1-ts ypk2*Δ and *tor1*Δ *tor2*Δ mutant strains, *SLM1* was expressed from the *GAL1* promotor as fusion proteins with a double HA epitope at the N-terminus (pAS25, *CEN URA3*). To analyze phosphorylation of the $Slm1_{\Delta CN}$ mutant, wild type and mutant Slm1 variants were expressed in strain W303 as N-

terminal TAP fusion proteins from a centromere-based plasmid under the control of the *GAL1* promotor. In all cases, cells were cultivated in raffinose-containing selective medium to an A_{600} of 1.0, followed by a 2 1/2-h galactose induction. Glucose was then added to 2 % final concentration to stop protein expression, and cells were incubated for another 30 min at 26˚C. Cells were then divided into 50 ml aliquots and heat shocked by incubation at 38˚C for the indicated periods of time. Cell extract preparation and TAP purification and analysis were performed as described above. HA-tagged Slm1 was purified from extracts of wild type and *pkh1ts pkh2*Δ mutant strains using anti-HA-sepharose affinity beads. Analysis of phosphorylation status of Slm fusion proteins was performed by Western blots using anti-phosphoserine (Q5) and anti-phosphothreonine (Q7) antibodies following essentially the manufacturer's protocol. Detection of tagged proteins by anti-HA or anti-TAP antibodies was as described previously (20). Western blots were sequentially probed with each antibody with stripping in-between. Western blots were developed using a commercial chemiluminescence detection system (Renaissance; PerkinElmer Life Sciences, Boston, MA) and x-ray film (Biomax MR; Eastman Kodak, Rochester, NY). Quantitation was performed in two ways. First, ECL Western blots were exposed to ECL reagents for various periods of time (10 sec to 8 min) and for each set of experiments (Control/PHS/Myriocin, Control/$CaCl_2$/BAPTA/FK506, and Control/$Slm1_{\Delta CN}$) the same exposures in the linear range were digitized and quantitated by densitometry using Image Gauge 4.0 program. Quantitation was also performed from samples that were independently analyzed by SDS-PAGE and by quantitative Western blot analysis using primary antibodies and Alexa Fluor IR680-conjugated anti-rabbit antibody. Blots were detected using Odyssey infrared imaging system (Licor Biosciences, Lincoln, NE). Both quantitation methods gave qualitatively the same result. However, it should be noted that between

independent experiments, some variability in the magnitude of change in phospho-serine/threonine levels using Q5/Q7 antibodies were observed that may reflect the differences in basal phosphorylation levels at zero time.

Expression and purification of proteins in *E. coli* and GST pull-down assays

All proteins were expressed in *E. coli* BL21(λDE3) as GST or 6His fusion proteins and purified on GSH-conjugated and Ni^{2+}-chelating agarose beads, respectively, following the manufacturer's instructions. *In vitro* transcription and translation and labeling of proteins with [^{35}S] Easy Tag Express Protein Labeling Mix (NEN Life Science Products) was performed using the Promega TNT T7 Quick Coupled transcription/translation system. *CNA1* cloned into vector TNT521 (20) were used as DNA template in the reactions. Pull-downs using radioactively labeled Cna1 and Slm1, Slm2 or deletion variants thereof were performed as described previously (20).

Proteomic Analysis of Slm1 phosphorylation

Mass spectrometric identification of Slm1 phosphorylation was done as described before (33) with a minor modification. TAP-Slm1 protein was purified from heat-shocked (90 min, 38˚C) wild type cells as described above, separated by SDS-PAGE, and visualized by Coomassie brilliant blue staining. The Coomassie-stained protein band was excised and destained with 50 mM ammonium bicarbonate solution in 50% methanol. Gel pieces were washed in HPLC water overnight, and digested with either 100 ng of trypsin or 100 ng of AspN in 50 mM NH_4HCO_3 (pH 8.5) for 4 h. After digestion, peptides were extracted by addition of 200 µl of acetonitrile and supernatants were dried in a Speed-Vac dryer (Thermo Savant, Holbrook, NY). Each sample was then dissolved in 20 µl of 5% methanol /95% water / 0.1% formic acid solution and injected into

Surveyor HPLC system (ThermoFinnigan, Waltham, MA) using autosampler. An 100 mm x 75 □m, C18 column (5 µm, 300 Å pore diameter, PicoFrit™, New objective, Woburn, MA) with mobile phases of A (0.1% formic acid in water) and B (0.1% formic acid in methanol) was used with a gradient of 10-80% of mobile phase B over 10 min followed by 80% B for 10 min at a flow rate of 200 nl/min. Peptides were directly eletrosprayed into the mass spectrometer (Finnigan LTQ™, ThermoFinnigan, San Jose, CA) using nano-spray source. LTQ were operated in the data-dependent mode acquiring fragmentation spectra of the top 20 strongest ions. All MS/MS spectra were searched against NCBI-nr protein sequence database with the specification of serine, threonine or tyrosine phosphorylation using the BioWorks database search engine (BioWorksBrowser ver 3.2, Thermo Electron, Waltham, MA). Phosphorylated peptides were identified based on stringent BioWorksBrowser filtering criteria (peptide probability > 5 X 10^{-5} and Xcorr score > 4.0) and were manually examined for consecutive b- or y- ions to eliminate false positives.

Immunofluorescence techniques and actin depolymerization

Cells were prepared for immunofluorescence experiments as described previously (20). GFP experiments in living cells were performed using cells grown in selective media (selecting for maintenance of chromosomally encoded or plasmid-borne fusions) and mounted for viewing in 1% low-melting agarose. To investigate a role of the actin cytoskeleton in Can1 plasma membrane delivery, cells expressing GFP-Can1 from a low-copy vector (40) were treated with latrunculin A (5µM) to depolymerize the actin cytoskeleton and Can1 localization was visualized after various times. All cells were viewed using a 100x plan oil-immersion lens (numerical

aperture 1.4). Images were acquired with the use of a DeltaVision deconvolution microscope (Applied Precision, Mississaugua, Ontario, Canada) and analyzed as described previously (20).

Scoring of actin cytoskeletal polarization

Actin polarization was examined in small- and medium-budded cells (~100-150 cells were analyzed in each case) as described previously. The actin cytoskeleton was considered polarized if six or fewer actin patches were localized in the mother cells and patches were concentrated at the bud neck and actin cables were polarized. Cells with the majority of actin patches polarized to the bud and the bud neck and containing polarized actin cables were classified as partially polarized. Cells with more actin patches in the mother cell than in the bud were classified as depolarized.

RESULTS

SLM1 deletion confers supersensitivity to myriocin

Previously we demonstrated that Slm1 and Slm2 localize to characteristic plasma membrane subdomains that are enriched in the H^+-ATPase Pma1 (20). Because Pma1 is a well-documented lipid raft protein (4), this raised the question whether Slm proteins are also components of raft-based microdomains and whether their function is modulated by sphingolipids. Myriocin sensitivity has often been used as a read-out to screen for and identify novel components of the sphingolipid signaling pathway in yeast (53). Myriocin blocks *de novo* synthesis of sphingolipids by specifically inhibiting Lcb1 (Figure 1), the enzyme that catalyzes the first committed step in sphingolipid biosynthesis. To begin to examine a potential relationship between Slm proteins and sphingolipids, we tested whether myriocin affects growth of yeast cells lacking *SLM1* or *SLM2*.

In agreement with earlier findings (53), myriocin inhibited the growth of wild type cells in a dose-dependent manner, with 2 μg/ml being the lowest concentration that can completely inhibit growth (data not shown). When compared to the wild type strain, the isogenic *slm1*Δ mutant strain was supersensitive to myriocin. The growth of the *slm1*Δ mutant was already severely delayed at myriocin concentrations as low as 0.25 μg/ml and was completely inhibited at 0.5 μg/ml (Figure 2A). In contrast, the growth of the wild type strain was normal under these conditions (Figure 2A and data not shown). Deletion of *SLM2* also conferred enhanced sensitivity to myriocin, but perhaps due to the much lower abundance of the Slm2 protein (3), the effect was far less pronounced (Figure 2A).

To determine whether myriocin-mediated growth inhibition is a direct consequence of sphingolipid depletion, we asked whether exogenous addition of PHS could rescue the myriocin supersensitivity of *slm1*Δ cells. PHS has been shown previously to reverse myriocin-mediated

growth inhibition (53) and, as shown in Figure 2B, addition of exogenous PHS to growth medium containing myriocin also restored growth to *slm1*Δ mutant cells. Thus, Slm1 is required for growth when *de novo* sphingolipid biosynthesis is compromised suggesting that Slm proteins function in a process that is modulated by intracellular sphingolipid concentration.

Genetic interaction between *slm1*Δ and mutants in the sphingolipid biosynthesis pathway

To further establish a functional relationship between Slm proteins and sphingolipids, we examined whether the combination of an *slm1*Δ mutation with mutations in sphingolipid biosynthetic genes results in synergistic effects and leads to synthetic sickness or lethality. To do this, heterozygous diploids were generated by crossing a *SLM1* deletion mutant strain with a panel of isogenic deletion mutations that block various nonessential steps in the sphingolipid biosynthesis pathway (Figure 1). The resulting diploid strains were then sporulated, and tetrads were dissected, allowed to germinate at 30°C on rich medium and analyzed for segregation of genetic markers.

Viable doubly mutant progeny were recovered in all crosses tested demonstrating that none of the double mutants combinations is synthetically lethal. However, *slm1*Δ conferred temperature-sensitive growth when combined with deletion mutations in three genes: *FEN1*, whose gene product regulates fatty acid elongation ((43), Figure 1), *LCB4*, which encodes the major sphingoid base kinase that phosphorylates DHS and PHS to DHS-1P and PHS-1P ((42), Figure 1), and *CSG2*, which is required for the mannosylation of inositolphosphorylceramide (IPC) to form the complex sphingolipid MIPC ((56, 61), Figure 1). Accordingly, when compared to single mutant and wild-type strains, colony formation and growth of *slm1*Δ *csg2*Δ*, slm1*Δ *fen*Δ*1,* and *slm1*Δ *lcb4*Δ double mutant strains was severely compromised at 38˚C, but was not

affected at 26˚C (Figure 3A). Attempts to test for synthetic lethality between *slm2*Δ and either *csg2*Δ, *fen1*Δ, or *lcb4*Δ, were unsuccessful because these diploid strains failed to sporulate (data not shown). Nevertheless, we conclude that loss of Slm1 confers temperature-sensitive growth when combined with mutations that affect sphingolipid biosysnthesis (3, 20). Because *de novo* sphingolipid biosynthesis is required for heat stress resistance (19, 32, 58), our findings suggest that Slm1 and sphingolipids play a common role required for survival under heat stress conditions.

Loss of sphingolipid synthesis results in defects in actin cytoskeletal organization (23, 60). Notably, these defects are similar to those previously reported for yeast mutants lacking Slm function (3, 20) suggesting that sphingolipids and Slm proteins may cooperate to regulate proper actin polarization. To investigate this hypothesis, we visualized actin in *slm1*Δ *csg2*Δ, *slm1*Δ *fen1*Δ and *slm1*Δ *lcb4*Δ double mutant cells by fluorescence microscopy using Alexa594-conjugated phalloidin. When shifted to 38˚C for 2 hr, all double mutant cells exhibited severe actin cytoskeletal defects. Actin patches were completely depolarized and distributed evenly between mother and daughter cells and actin cables were either faint or completely absent (Figure 3B). In contrast, actin cytoskeletal organization in the single mutant cells was similar to wild type, with actin cables traversing from mother to bud and actin patches polarized toward the bud tip (Figure 3B). Consistent with the temperature-sensitive growth of the double mutants, actin polarization defects were also temperature-dependent and only observed at 38˚C, but not at 26˚C (data not shown). Taken together, these data indicate that Slm proteins and sphingolipids play a redundant role in promoting cell growth and proper actin polarization during heat stress conditions.

Depletion of cellular sphingolipid levels only weakly affects Slm1 plasma membrane association

Sphingolipid biosynthesis is required for plasma membrane localization of lipid raft associated proteins (4, 40). Because Slm1 and Slm2 showed partially overlapping localization with multiple lipid raft-associated proteins, including Pma1, Can1 and Sur7 ((20), Supplementary Figure 1), this raised the question whether sphingolipid synthesis was also required for Slm1 and Slm2 plasma membrane association (3, 20). To investigate this possibility, we examined the subcellular localization of an Slm1-GFP fusion protein, expressed under control of its endogenous promoter, in cells treated with various concentrations of myriocin. These experiments showed that Slm1-GFP localization to punctate foci at the plasma membrane was not noticeably affected when cells were incubated at 26˚C in the presence of up to 2μg/ml myriocin (data not shown). A moderate decrease in plasma membrane Slm1-GFP signal was observed when cells were exposed to toxic concentrations of myriocin (2 μg/ml) in combination with mild heat shock treatment (3 hrs at 38˚C data not shown) suggesting that sphingolipids, in part, are required for Slm targeting to the plasma membrane under heat stress conditions. However, even under these conditions, a significant portion of GFP-Slm1 was still observed in punctate foci at the plasma membrane (data not shown). In addition, HA-Slm1 localized normally to the plasma membrane in the temperature-sensitive *lcb1-100* mutant (data not shown), which is defective for sphingolipid biosynthesis (26). Taken together, our data suggest that sphingolipids are dispensable for Slm plasma membrane association under regular growth conditions and only moderately affect Slm1 plasma membrane targeting under heat stress conditions, thus raising the possibility that sphingolipids modulate Slm function by an additional mechanism.

Sphingolipids modulate Slm1 and Slm2 phosphorylation in response to heat stress

Slm1 and Slm2 are phosphoproteins *in vivo* and previous studies have demonstrated that Slm proteins are dephosphorylated immediately following heat shock and become rephosphorylated during the recovery period (3). Because *de novo* sphingolipid synthesis is transiently upregulated during heat stress conditions, we wished to determine whether sphingolipids affect Slm phosphorylation. To this end, strains containing chromosomally integrated TAP-tagged Slm1 and Slm2 were grown to mid-logarithmic phase in YPD medium at 26˚C, separated into aliquots and either shifted to 38˚C for various periods of time or left at 26˚C. Cell extracts were then prepared and TAP-tagged Slm1 and Slm2 were purified by IgG-sepharose affinity purification, separated by SDS-PAGE and detected by immunoblotting using anti-TAP antibodies or antibodies that specifically recognize phospho-serine (Q5) and phospho-threonine (Q7) residues.

As shown in Figure 4A, Slm1 produced prominent Q5/Q7-immunoreactive bands of the expected molecular weight for Slm1-TAP suggesting that Slm1 is phosphorylated on both serine and threonine residues. The intensity of Q5 and Q7 signals immediately following heat shock (5-10 min) either did not change or weakly decreased (Q5: Figure 4C). However, a significant increase in Q5 and Q7 signal intensity was observed later during heat shock suggesting that Slm1 phosphorylation on serine and threonine residues is stimulated during the recovery period (Figure 4A and C). Slm2 also produced Q5/Q7 immunoreactive bands (Figure 4B). However, due to the approximately 10-fold lower abundance of Slm2 protein in wild type cell extracts, the Q5/Q7 signals were weak and difficult to quantitate reproducibly (Figure 4B and C; note that exposure times of Western blots shown are 8-fold longer than with Slm1) and our subsequent analysis thus mainly focused on Slm1. Nevertheless Slm2 phosphorylation modestly increased

during heat shock, as judged by increases in Q5 and Q7 signal intensity (Figure 4B and C). Taken together, our data are in good agreement with earlier studies (3) and demonstrate that Slm1 and Slm2 phosphorylation on serine and threonine residues is stimulated in response to heat shock.

To examine whether the phosphorylation status of Slm1 and Slm2 is modulated by sphingolipids, cells were preincubated with myriocin (2 μg/ml final concentration) for 30 min at RT to block cellular sphingolipid synthesis and were then shifted to 38˚C. Protein extracts were prepared after various periods of time and Slm1-TAP and Slm2-TAP were isolated, separated by SDS-PAGE, and probed with anti-TAP, Q5 and Q7 antibodies. Myriocin treatment completely abolished the heat-induced increase in Q5 and Q7 immunoreactive bands and, over time, decreased Q5 and Q7 signals below basal levels (Figure 4) indicating that *de novo* sphingolipid synthesis is essential for stimulating Slm1 and Slm2 phosphorylation during heat stress. Consistent with a role of sphingolipids in promoting Slm phosphorylation, we found that pretreatment of cells with exogenous PHS (10 μM) for 30 min before heat shock significantly increased basal levels of Slm1 and moderately increased Slm2 phosphorylation compared to control cells as judged by the intensity of Q5 and Q7 signals (Figure 4). PHS also enhanced phosphorylation of Slm1 during early periods of heat shock. Together, our data argue that the stimulation of Slm phosphorylation on serine and threonine residues observed in response to heat stress is mediated by an increase in *de novo* sphingolipid synthesis.

Calcineurin dephosphorylates Slm proteins during heat stress

Genome-wide two-hybrid studies demonstrated that Slm2 interacts with Cna1 and Cna2 (31, 57), the catalytic subunits of the Ca^{2+}/calmodulin-dependent serine/threonine protein phosphatase

calcineurin (13). These findings suggested that Slm2, and possibly Slm1, may be a substrate of calcineurin and dephosphorylated *in vivo*. In support of such a hypothesis, potential calcineurin binding sites that fit the consensus binding motif PxIxIT/Q (12, 38) are present in the extreme C-terminal regions of both Slm1 (amino acids 668-682) and Slm2 (amino acids 636-649; Figure 5A).

To confirm the two-hybrid interaction between Slm2 and calcineurin subunits, we performed *in vitro* pull-down assays using recombinant purified 6His-tagged Slm1 and Slm2 fusion proteins and [^{35}S]-labeled Cna1 generated by a coupled transcription/translation reaction. As shown in Figure 5B, Cna1 was readily recovered on agarose beads containing bound 6His-Slm1 and 6His-Slm2, but not on resin alone. In contrast, Slm1 and Slm2 mutants lacking the potential C-terminal calcineurin-binding domain failed to retain Cna1 (Figure 5B). Thus Slm1 and Slm2 directly associate with Cna1 suggesting that Slm1 and Slm2 are novel targets of calcineurin.

To explore whether Slm1 and Slm2 are regulated by calcineurin *in vivo*, we monitored Slm phosphorylation during heat stress under conditions that activate or inactivate calcineurin. Birchwood and colleagues previously showed that heat shock or exogenous PHS stimulate Ca^{2+} influx via the plasma membrane Cch1 channel resulting in accumulation of intracellular Ca^{2+} and activation of calcineurin (7). They further demonstrated that calcineurin activation can be stimulated by high extracellular Ca^{2+} concentrations and blocked by the membrane-impermeable Ca^{2+} chelator BAPTA. To determine whether Slm proteins are substrates for calcineurin during heat stress, we monitored Slm1 and Slm2 phosphorylation in yeast cells pretreated with $CaCl_2$ (100 mM) or BAPTA (10 μM) for 30 min prior to heat shock. Compared to control-treated yeast cells, Q5/Q7 immunoreactive Slm1 (Figure 5C, D) and Slm2 (data not shown) signals were

significantly decreased at all time points in extracts derived from cells challenged with high concentrations of extracellular Ca^{2+}. Conversely, blocking Ca^{2+} influx by pretreatment of yeast cells with BAPTA significantly enhanced Slm1 and Slm2 phosphorylation (Slm1: Figure 5C, D; Slm2: data not shown), as judged by the increase in Q5 and Q7 signal intensities. Importantly, BAPTA significantly stimulated basal phosphorylation and also enhanced Slm phosphorylation immediately following heat shock. Taken together, our results demonstrate that Slm phosphorylation is downregulated in response to Ca^{2+} influx, possibly by activation of a Ca^{2+}-activated phosphatase that counteracts heat-induced phosphorylation.

To determine whether Slm dephosphorylation is mediated by calcineurin, we pretreated cells with the immunosuppressive drug FK506, which is a specific inhibitor of calcineurin (36). FK506 treatment caused a noticeable increase in basal Slm1 phosphorylation on serine and threonine residues and also enhanced phosphorylation during the early phases of heat shock compared to control-treated cells (Figure 5C, D), but did not affect maximal phosphorylation levels. To determine whether Slm1 is an *in vivo* substrate of calcineurin, we compared serine and threonine phosphorylation levels of wild type Slm1 and the $Slm1_{\Delta CN}$ mutant that lacks the C-terminal calcineurin-binding site. Both proteins were expressed in wild type cells as N-terminal TAP fusion proteins from the galactose-inducible *GAL1* promoter and were then purified and analyzed by Western blotting using Q5 and Q7 antibodies. As shown in Figure 5E and F, the serine and threonine phosphorylation of $Slm1_{\Delta CN}$ was increased compared to that of wild-type Slm1 in the absence of heat stress stimulation and remained increased over wild type during early phases of heat treatment. These data demonstrate that Slm proteins are substrates of the protein phosphatase calcineurin and suggest that calcineurin counteracts Slm phosphorylation when cells are grown at physiological temperatures and immediately following heat shock.

Collectively, our data argue that Slm proteins are subject to both positive and negative control by kinases and phosphatases in response to cellular stress.

To better understand the physiological role of calcineurin and sphingolipid-mediated regulation of Slm, we next investigated whether the temperature-sensitive growth of an *slm1-ts slm2*Δ mutant strain (JK515) could be rescued by addition of FK506 or PHS to the growth medium. As shown in Figure 6, FK506 and PHS, when added together, were able to partially restore growth at the nonpermissive temperature, whereas little effect was observed when FK506 and PHS were added alone. One interpretation of these results is that calcineurin and sphingolipids antagonistically regulate Slms with calcineurin-mediated dephosphorylation inhibiting and PHS stimulating Slm function. Thus, by simultaneously providing the stimulatory signal and blocking calcineurin-mediated inhibition, Slm activity may be maximally enhanced. In agreement with such a hypothesis, we found that growth and actin defects of *slm1*Δ *csg2*Δ, *slm1*Δ *fen1*Δ and *slm1*Δ *lcb4*Δ double mutants at 38˚C could be significantly suppressed by the combined addition of PHS and FK506 to the growth medium, whereas addition of either reagent alone was less effective (Supplementary Figure 2).

Slm1 phosporylation involves the sphingolipid-activated kinases Pkh1 and Pkh2

Previous studies identified the functionally redundant protein kinases Pkh1 and Pkh2 as effectors of sphingolipid signaling and demonstrated that the two kinases are directly activated *in vitro* by nanomolar concentrations of sphingoid bases (22, 29). To determine whether Slm1 phosphorylation is dependent on Pkh1/2, we expressed HA-tagged *SLM1* under the control of the *GAL1* promoter from a low-copy vector in wild type and temperature sensitive *pkh1-ts pkh2*Δ mutant cells. HA-Slm1 synthesis was induced at 26˚C for 2 hr in the presence of galactose, and

then glucose was added to shut off further expression. After a 30 min incubation, cells were shifted to the nonpermissive temperature (38˚C) and Slm1 phosphorylation was examined using Q5 and Q7 phospho-specific antibodies. As expected, there was a pronounced increase in phospho-serine and phospho-threonine levels of Slm1 during the course of heat shock treatment of wild type cells (Figure 7). In contrast, *pkh1-ts pkh2*Δ cells showed reduced basal and heat-induced phosphorylation on serine and threonine as determined by the levels of intensity of the Q5 and Q7 signals (Figure 7). While there was an initial weak increase in Q5 and Q7 signals following shift to 38˚C, likely due to residual Pkh activity, the increase in Q5 and Q7 signals typically observed after longer incubation at 38˚C (30-90 min) was abrogated in *pkh1-ts pkh2*Δ cells (Figure 7). These results suggest that Slm1 phosphorylation on serine and threonine residues is at least partially regulated by the sphingoid base-dependent Pkh signaling cascade during heat stress and that the Pkh kinases may be upstream regulators of the Slm pathway.

To determine whether Pkh kinases directly phosphorylate Slm proteins, we expressed Pkh1 as a 6His fusion protein in *E. coli*, purified the recombinant protein and tested whether it could phosphorylate recombinant GST-Slm1 or GST–Slm2 in an *in vitro* kinase assay as described (37). However, while efficient Pkh1 autophosphorylation was observed, no phosphorylation of Slm1 or Slm2 was detected (data not shown). Thus, Slm1 and Slm2 phosphorylation is indirectly modulated by Pkh kinases.

Pkh1 and Pkh2 phosphorylate and activate a pair of redundant protein kinases termed Ypk1 and Ypk2 that are essential for growth and the regulation of cell wall integrity and actin cytoskeleton polarization (9, 46, 47). PHS can directly stimulate these kinases or activate them indirectly via Pkh1/2 (37). To determine whether Slm1 phosphorylation involves Ypk kinases, we expressed *HA-SLM1* in the temperature-sensitive *ypk1-ts ypk2* mutant strain and measured

phospho-Slm1 levels during heat shock treatment. In contrast to cells lacking Pkh activity, yeast mutants defective in Ypk1/2 showed no apparent defect in the rate of heat-induced Slm phosphorylation (Figure 7). Heat-induced increases in Q5/Q7 signals were also observed in cells containing a temperature-sensitive mutation in the Tor2 kinase (Figure 7), which was previously shown to phosphorylate Slm1 *in vitro* and *in vivo* (3, 20). Thus, heat stress-induced phosphorylation of Slm1, at least as visualized by Q5 and Q7 antibodies, appears to involve Pkh, but not Ypk or Tor2 kinases.

Phosphorylation of Ser659 is essential for Slm1 function under heat stress conditions

To gain insight into how Slm activity is affected by phosphorylation, we next undertook to identify phosphorylation sites in Slm1. Slm1-TAP protein expressed under control of its endogenous promoter was purified from cells incubated at 38˚C for 90 min to stimulate Slm1 phosphorylation. Purified Slm1-TAP was then resolved by SDS-PAGE and visualized by staining with Coomassie brilliant blue. The band corresponding to Slm1-TAP was extracted from the gel, subjected to tryptic proteolysis and analyzed by mass spectrometry (see Materials and methods). Analysis of the MS/MS spectra identified 22 predicted Slm1 tryptic peptides containing a common phospho-serine site, T_{653}NTSMSS(p)LPDT, with Xcorr scores of >4.0 (data not shown) suggesting that this residue represents a major site of phosphorylation. No other candidate phosphorylation sites were detected. Ser_{659} is conserved in Slm2 (corresponding to Ser_{626}) and immediately precedes the calcineurin binding site (amino acids 668-682).

To probe the potential function of Ser_{659} phosphorylation, we generated a phosphorylation site-defective Slm1 mutant ($Slm1_{S659A}$) in which Ser_{659} was substituted with Ala. To confirm that this single amino acid change affects heat-induced phosphorylation, we first

expressed the $Slm1_{S659A}$ mutant as a HA-tagged protein in wild type cells, subjected cells to heat shock treatment and analyzed the purified HA-$Slm1_{S659A}$ protein for phosphorylation using Q5 and Q7 antibodies. Immunoblotting with anti-TAP and Q7 antiserum revealed similar levels of TAP immunoreactivity in the $Slm1_{S659A}$ mutant as in the corresponding wild type protein and, in both cases, the expected increase in Q7 signals in response to heat shock treatment was observed (Figure 8A). In contrast, immunoblotting with Q5 antiserum revealed only basal levels of Slm1 phosphorylation, whereas the typical heat-induced increase in Q5 signal was completely abrogated in the $Slm1_{S659A}$ mutant (Figure 8A). Together, these experiments confirm that Ser_{659} is indeed the major serine residue phosphorylated during the heat stress response and that mutagenesis of this site specifically affects serine, but not threonine phosphorylation during heat treatment.

To test whether phosphorylation at Ser_{659} is required for Slm1 activity, we employed a plasmid-shuffling assay. An *slm1*Δ *slm2*Δ double mutant strain carrying a *SLM1 URA3* plasmid (strain JK520) was transformed with a second plasmid containing *LEU2* as a marker and containing either wild type *SLM1*, or the mutant $SLM1_{S659A}$ variant. Transformants were then streaked on solid medium containing 5-fluoroorotic acid (5-FOA) to counter select the *SLM1 URA3* plasmid. We found that *LEU2* plasmids (vector p425GPD) containing either wild type *SLM1* or $SLM1_{S659A}$ could complement the lethality of *slm1*Δ *slm2*Δ null mutant cells on 5-FOA-containing medium at 30˚C (Figure 8C). However, only the *LEU2* plasmid containing wild type *SLM1*, but not $SLM1_{S659A}$ was able to confer growth at 38˚C (Figure 8C). As expected, the *slm1*Δ *slm2*Δ double mutant transformed with a *LEU2* plasmid containing the inactive $SLM1_{\Delta C}$ mutant (20) was unable to grow on 5-FOA-containing medium at any temperature (Figure 8C). We thus

conclude that phosphorylation of Slm1 at Ser_{659} is dispensable for growth under normal growth conditions, but is essential for survival under heat stress conditions.

SLM1 overexpression partially rescues growth and actin defects of cells lacking Pkh function

Because our biochemical data suggested that Pkh1/2 kinases are required for Slm1 phosphorylation, we wanted to explore what role Slm1 plays in Pkh1/2 signaling and whether phosphorylation at Ser_{659} confers enhanced Slm1 activity. To do this we mutated Ser_{659} in Slm1 to aspartate (yielding $Slm1_{S659D}$), because the introduction of an acidic charge often mimics phosphorylation. Galactose-induced expression of $SLM1_{S659D}$ from a low-copy plasmid (pAS25) rescued the temperature-sensitive growth of the *slm1-ts slm2*Δ mutant at 38˚C, in contrast to $SLM1_{S659A}$ (data not shown), demonstrating that $Slm1_{S659D}$ is functional.

$SLM1_{S659D}$ or wild type *SLM1* were then expressed in the *pkh1-ts pkh2*Δ mutant and tested for their ability to suppress the lethality of this mutant at the nonpermissive temperature. As expected, upon shifting to 38˚C, growth was fully restored to *pkh1-ts pkh2*Δ mutant cells when *PKH1* was expressed from a low-copy plasmid (YCpG22-*PKH1)* under control of the *GAL1* promoter (data not shown). In contrast, vector alone or expression of wild type *SLM1* or $SLM1_{S659D}$ resulted in no or only very slight restoration of growth (data not shown). However, Pkh1 and Pkh2 are involved in the regulation of multiple essential cellular functions, required for cell wall integrity and actin polarization. It was possible, then, that Slm proteins regulated only a subset of Pkh1-dependent essential functions. Indeed, microscopic examination of *pkh1-ts pkh2*Δ cells expressing *SLM1* revealed predominantly cell ghosts, suggesting that *SLM1* is unable to suppress the cell lysis defect of the *pkh1-ts pkh2*Δ mutant. To test whether *SLM1* suppresses the

growth defect of *pkh1-ts pkh2*Δ cells in the presence of osmotic support, galactose plates were supplemented with 1 M sorbitol and growth of transformants was assessed at 38˚C. As shown in Figure 9A, growth of the temperature sensitive *pkh1-ts pkh2*Δ mutant transformed with empty vector was severely delayed at 38˚C (Figure 9A). Under these conditions expression of $SLM1_{S659D}$ partially rescued the slow growth defect of the *pkh1-ts pkh2*Δ mutant, although not as strongly as *PKH1* (Figure 9A). Interestingly, expression of the $SLM1_{\Delta CN}$ mutant, which lacks the calcineurin-binding site, also suppressed the growth defect in a manner similar to $SLM1_{S659D}$ and consistently better than wild type *SLM1* (Figure 9A).

Taken together, one reasonable explanation for our results is that the Pkh signaling cascade increases basal activity of Slm1 by promoting Slm phosphorylation and that this increase in activity is important for survival under heat stress and the repolarization of actin cytoskeleton. If this were true, we would anticipate that the growth defect of the *pkh1-ts pkh2*Δ mutant was also suppressed by the exogenous addition of PHS and FK506, as this treatment is expected to result in increased Slm phosphorylation and enhanced Slm function. As shown in Supplementary Figure 3, we found that this was indeed the case as combined addition of PHS and FK506 to the growth medium significantly restored growth to *pkh1-ts pkh2*Δ mutant cells at the restrictive temperature of 34˚C in the absence of osmotic stabilization, whereas addition of PHS or FK506 alone was less effective (Supplementary Figure 3).

To investigate the role of Slm1 in Pkh signaling further, we assayed the ability of Slm1 wild type and mutant variants to suppress the actin polarization defect of the *pkh1-ts pkh2*Δ mutant (46). To investigate whether Slm1 can restore proper actin polarization, *pkh1-ts pkh2*Δ mutant cells containing plasmids expressing *PKH1* or wild type and mutant *SLM1* variants were grown at 26°C in medium osmotically stabilized with 1M sorbitol and containing galactose to

induce expression of *PKH1* and *SLM1*, respectively. Cells were then shifted to 38°C for 2 hr and processed for visualization of the actin cytoskeleton. *pkh1-ts pkh2*Δ cells containing vector alone exhibited the expected random distribution of actin patches and lacked actin cables after incubation at 38˚C for 2 hr, even when grown in the presence of 1 M sorbitol (Figure 9B and C). In contrast, *pkh1-ts pkh2*Δ cells expressing *PKH1* under the control of the *GAL1* promoter displayed the normal cell cycle-dependent polarized distribution of actin patches and cables (Figure 9B and C). Actin polarization could also be significantly restored in *pkh1-ts pkh2*Δ cells by expression of $SLM1_{S659D}$ and, to a slightly lesser degree by expression of $SLM1_{\Delta CN}$ (Figure 9B and C). Likewise, overexpression of wild type *SLM1* rescued the actin polarization defects of *pkh1-ts pkh2*Δ cells, although less efficiently than $SLM1_{S659D}$ and $SLM1_{\Delta CN}$ (Figure 9B and C). Taken together, these data suggest that Slm proteins can provide a subset of essential Pkh-dependent functions involved in maintaining or restoring proper actin polarization.

Loss of Slm function results in mislocalization of the arginine permease Can1

Sphingolipids, in conjunction with sterols, are also involved in the transport of lipid raft-associated proteins to the plasma membrane. In particular, the targeting of plasma membrane H^+-ATPase Pma1 (4) and the arginine permease Can1 (40) to plasma membrane rafts was shown to be dependent on sphingolipid and ergosterol synthesis. Depletion of either of these raft lipids in *lcb1-100* or *erg24*Δ mutants abolished the transport of Pma1 and Can1 to the surface and resulted in their accumulation in intracellular compartments (3, 37).

To further explore a role of Slm1 and Slm2 in sphingolipid-dependent processes, we investigated whether trafficking of Pma1 and Can1 was affected in the *slm1-ts slm2*Δ mutant. The localization of Pma1 was examined by indirect immunofluorescence using anti-Pma1

antibodies. To follow the localization of Can1, wild type and *slm* mutant cells were transformed with a low-copy centromer-based plasmid (pCAN1-GFP) that produced Can1 as a fusion protein to GFP and the GFP signal was monitored in living cells. Pma1 and Can1 localization was compared in wild type and *slm1-ts slm2*Δ cells grown either at the permissive temperature or shifted to 38˚C for 2 hr. Pma1 appeared similarly localized to the plasma membrane in wild type and *slm1-ts slm2*Δ mutant cells (data not shown), suggesting that Slm proteins are not required for Pma1 trafficking. Can1-GFP, when expressed in wild-type cells exclusively localized to the plasma membrane at both permissive and nonpermissive temperatures and exhibited the characteristic punctate fluorescence pattern typical for a lipid raft-associated protein (Figure 10A). In contrast, Can1 targeting to the plasma membrane was partially defective at the permissive temperature (observed in 70% of cells) in *slm1-ts slm2*Δ cells and completely defective (observed in 95% of cells) when cells were shifted to the nonpermissive temperature for 2 hr. Under these conditions, Can1 accumulated in a perinuclear compartment and in areas adjacent to the plasma membrane (Figure 10A). Consistent with previous reports (40), intracellular accumulation of Can1 was also observed in the *erg24*Δ mutant (100% of cells), which lacks the raft lipid ergosterol and is known to accumulate Can1 in the peripheral and perinuclear ER (40), and in the *lcb1-100* mutant, which accumulates Can1 in the ER and the Golgi (26˚C: 93% of cells; 38˚C: 100% of cells; Figure 10A). Expression of wild type *SLM1* in *slm1-ts slm2*Δ cells significantly prevented the intracellular accumulation of Can1 at both permissive and nonpermissive temperatures, indicating that the defect in Can1 targeting is due to decreased Slm activity (Figure 10B). The retention of Can1 in the ER could also be partially reversed by treatment of *slm1-ts slm2*Δ cells with PHS and FK506 (Figure 10B).

Interestingly, mislocalization of Can1-GFP to perinuclear and peripheral ER

compartments was also observed in the *pkh1-ts pkh2*Δ strain at both permissive (observed in 65% of cells) and nonpermissive temperatures (observed in 92% of cells; Figure 10A) raising the possibility that Pkh-dependent regulation of Slm proteins is required for Can1 trafficking. Consistent with such a hypothesis, overexpression of *SLM1* when combined with FK506 treatment of *pkh1-ts pkh2*Δ cells partially prevented the ER accumulation of Can1 (Figure 10C).

Mutants that affect Can1 activity or its transport to the plasma membrane have been shown to confer increased resistance to arginine analog canavanine, which is toxic to yeast (44). Thus if loss of Slm function indeed affects Can1 trafficking to the plasma membrane, we would expect to observe a decrease in arginine uptake and a corresponding decrease in canavanine sensitivity. To examine this point, dilution series of wild-type and *slm1-ts slm2*Δ cultures were spotted on a plate containing 0.5 μg/ml canavanine and assayed for their ability to grow at 30˚C. The parental wild type strain W303 contains an endogenous mutation in the *CAN1* gene and showed growth at all dilutions on medium containing canavanine (Figure 10D). However, transformation of W303 with the low-copy *GFP-CAN1* plasmid rendered cells canavanine sensitive (Figure 10D). In contrast, the *slm1-ts slm2*Δ transformed with *GFP-CAN1* was resistant to canavanine, although not as strongly as the *lcb1-100* mutant (Figure 10D). Because *slm1-ts slm2*Δ and *lcb1-100* mutants appear to accumulate Can1 in intracellular compartments, it is reasonable to assume that canavanine resistance is due to decreased canavanine uptake through Can1.

Because loss of Slm and Pkh function disrupts proper actin polarization, we next investigated whether the defect in Can1 trafficking observed in these mutants could be due to a defect in actin assembly. To do this, Can1-GFP localization was examined in wild type cells treated with the drug latrunculin A, which rapidly depolymerizes actin. Consistent with previous

reports, we found that latrunculin A did not cause Can1-GFP delocalization from the plasma membrane (Figure 10E; (39)). However, transport of newly synthesized Can1 from the ER to the plasma membrane was disrupted or delayed upon blocking actin assembly, because Can1-GFP signal accumulated in the ER, and to a lesser degree on the Golgi over a treatment period of 120 min (Figure 10E). Consistent with the hypothesis that Can1 transport is dependent on proper actin organization, intracellular retention of Can1 in the ER and the Golgi was also observed in temperature-sensitive *stt4*, *mss4* and *tor2* mutants (data not shown), which exhibit actin defects at the nonpermissive temperature (2, 16, 48). Taken together, these data indicate that Slm proteins are required for efficient ER to plasma membrane trafficking of the lipid raft-associated permease Can1, possibly by promoting proper actin polarization.

DISCUSSION

The related PH domain containing proteins Slm1 and Slm2 have been originally identified as effectors of the $PI4,5P_2$ and TORC2 signaling pathways and shown to be essential for growth and actin polarization (3, 20). The studies presented here extend these earlier observations and demonstrate that Slm proteins are also targets of sphingolipid-dependent signaling. We show that Slm1 is essential for growth and proper actin polarization under conditions when *de novo* sphingolipid synthesis is compromised, suggesting that Slm proteins and sphingolipids cooperate to promote cell survival. Our results further establish a role for sphingolipid signaling pathways in modulating Slm function during heat stress conditions. One role of sphingolipids may be to indirectly modulate Slm activity by regulating $PI4,5P_2$ synthesis required for Slm1 and Slm2 plasma membrane targeting (34). However, a second, essential role of the sphingolipid-activated signaling pathway is to stimulate Slm phosphorylation on both serine and threonine residues and this phosphorylation event is vital for survival under heat stress conditions.

Sphingolipids signaling is specifically induced in response to heat stress in yeast and the kinetics of Slm phosphorylation correlate well with heat-induced changes in sphingoid base metabolites. Heat stress induces a rapid increase in the sphingoid bases PHS and DHS. This increase is transient and peaks after 10 to 15 minutes, returning to basal levels within 60 min (19, 32). PHS and DHS are rapidly metabolized to PHS-1P and DHS-1P, which peak 15 min after heat stress (21, 52) followed after approximately one hour by an increase in ceramide metabolites via *de novo* synthesis (58). Thus, PHS or a PHS metabolite may promote Slm phosphorylation by activating an upstream kinase. Consistent with such an idea, we found that Slm phosphorylation levels are significantly diminished in a yeast mutant defective for the sphingoid base-activated kinases Pkh1 and Pkh2 suggesting that the Pkh signaling cascade

regulates Slm function. Slm1 and Slm2 lack canonical consensus Pkh/PDK1 phosphorylation motifs that are present in all known Pkh targets (9, 29). In agreement with this, Pkh1 failed to directly phosphorylate Slm proteins *in vitro*. Thus, Slm1 and Slm2 phosphorylation involves an as-yet unidentified kinase whose activity is modulated by the Pkh signaling cascade. Pkh kinases are known to directly activate several kinases including Pkc1p, Sch9, and the related Ypk1 and Ypk2. Our data thus far exclude Ypk1/2 and it remains to be determined which kinase(s) directly phosphorylates Slm1/2.

Heat-induced Slm1 phosphorylation is, at least in part, counteracted by the Ca^{2+}/calmodulin-dependent protein phosphatase calcineurin. We show that Slm1 and Slm2 both physically interact with Cna1 via a calcineurin docking site present in their C-termini and that deletion of this calcineurin binding site in Slm1 or treatment of yeast cells with the calcineurin inhibitor FK506 increases basal levels of Slm phosphorylation on both serine and threonine residues. Interestingly, calcineurin activation in an early phase of the heat shock response may also be mediated by sphingolipids (PHS-1P) through stimulation of Ca^{2+} influx. Thus, sphingolipids may modulate Slm phosphorylation both positively and negatively during heat stress. PHS-1P may trigger calcineurin-dependent dephosphorylation of Slm observed immediately following heat shock, whereas PHS stimulates Pkh-dependent rephosphorylation of Slm proteins during the recovery period. Together our data suggest that Slm activity is modulated via a phosphorylation/dephosphorylation cycle with Pkh kinases and calcineurin antagonistically regulating Slm activity.

How does phosphorylation/dephosphorylation affect Slm function? The finding that the specific calcineurin inhibitor FK506 in combination with PHS can partially suppress the growth defect of the temperature-sensitive *slm1-ts slm2*Δ mutant at the nonpermissive temperature

argues for a negative role of calcineurin in Slm regulation and a positive role of sphingolipids in enhancing Slm activity. Consistent with a negative role of calcineurin in Slm regulation, deletion of the calcineurin-binding site does not abolish Slm function. Accordingly, the $Slm1_{\Delta CN}$ mutant is not only functional and suppresses growth and actin defects of *slm1-ts slm2*Δ mutant cells at 38˚C (data not shown), but it is also more effective than wild type *SLM1* in restoring proper actin polarization in *pkh* mutant cells.

Our data further demonstrates that phospho-Slm plays a critical role during heat stress and is required for maintaining cell survival and proper actin polarization. This conclusion is supported by biochemical and genetic data showing that conditions that enhance Slm phosphorylation (treatment of cells with FK506 and PHS) also suppress the lethality and actin defects associated with loss of Slm function. Furthermore, identification and functional characterization of one heat-induced phosphorylation site in Slm1, Ser_{659}, using mass spectroscopic analysis and mutagenesis studies directly implicates phosphorylation in survival under heat stress. Substitution of Ser_{659} in Slm1 with Ala, which prevents phosphorylation, affects Slm1 function under heat shock conditions only. Accordingly, while this Slm1 variant can complement lethality of the *slm1-ts slm2*Δ mutant under physiological growth conditions (30˚C), it fails to do so at 38˚C. Thus, phosphorylation may increase Slm1 activity or promote interaction with a cellular component necessary for maintaining growth and proper actin polarization under environmental stress conditions. In agreement with such a hypothesis, the $Slm1_{Ser659D}$ mutant appears to be hyperactive *in vivo* compared to the wild type protein. Due to the close proximity of Ser_{659}, to the calcineurin binding site (amino acids 668-682), it is tempting to speculate that Ser_{659} is the site dephosphorylated by calcineurin. Further studies, however, are

needed to determine the identity of the residues dephosphorylated by calcineurin and its relation to Ser_{659}.

Sphingolipid-dependent activation of the Pkh pathway is essential for growth and activated Pkh kinases modulate at least two essential signaling branches required for cell wall synthesis and actin polarization. Our genetic and biochemical studies suggest that Slm proteins function as effectors in one Pkh-regulated signaling branch, or act in a parallel, functionally redundant pathway. Perhaps more in favor of the former, we found that increased dosage of *SLM1* can partially rescue the growth and actin cytoskeleton organization defects of the temperature-sensitive *pkh1-ts pkh2*Δ cells when these cells are osmotically stabilized. Conversely, increased dosage of *PKH1* neither suppressed the growth nor actin defects of the *slm1-ts slm2*Δ mutant at nonpermissive temperature (data not shown). In agreement with the notion that the Pkh signaling cascade stimulates Slm activity, mutations that enhance or mimic phosphorylation ($Slm1_{Ser659D}$ and $Slm1_{\Delta CN}$), confer enhanced ability to suppress the growth and actin defects of *pkh1-ts pkh2*Δ mutant cells. Together, our data are best compatible with a model in which Slm proteins function in a branch of the Pkh signaling pathway to promote actin polarization during heat stress.

Finally our studies suggest that Slm proteins are required for aspects of sphingolipid-dependent transport processes, because delivery of the arginine permease Can1 to the plasma membrane, which is dependent on *de novo* sphingolipid synthesis, is blocked in cells lacking Slm activity. In yeast, ongoing sphingolipid biosynthesis is required for the formation of lipid raft domains in the ER and may play a role in the fusion of COPII vesicles with *cis*-Golgi membranes (51). The defect in ER exit of Can1 in *slm-ts* mutants would thus be consistent with a common role of Slm proteins and sphingolipids in protein delivery to lipid raft microdomains.

Interestingly, plasma membrane delivery of the lipid-raft-associated protein Pma1 appeared not to be significantly affected in *slm1-ts slm2*Δ mutants. The reason for the intracellular retention of Can1 only is currently unknown, but may be due to the preferential association of Can1 and Pma1 with raft domains of different lipid compositions along the secretory pathway (45) and at the plasma membrane (39). Can1 is thought to associate with raft domains in the ER (45), whereas Pma1 raft association has been proposed to predominantly occur in the Golgi apparatus (4, 35). Thus, Can1 and Pma1 may be transported via different subpopulations of vesicles that are differentially sensitive to loss of Slm function. In support of such a hypothesis, immunofluorescence studies revealed more significant overlap of Slm1 signal with Can1 and Sur7, compared to Pma1 (Supplementary Figure 1). Thus Slm proteins may play a role in the trafficking of Can1/Sur7 containing vesicles and their targeting to specific membrane domains at the plasma membrane. Additional studies will need to address this issue.

Slm1 and Slm2 were previously implicated in vesicular trafficking to the cell surface, and several proteins, including the Rab-type GTPase Sec4 and the v-SNARE Snc1, necessary for fusion of secretory vesicles with the plasma membrane, were mislocalized in *slm1-ts slm2*Δ mutants (3). While the precise role of Slm proteins in the exocytotic pathway is not known, there is precedence for a functional connection between Snc1, and sphingolipid biosynthesis in this process. Sphingoid bases and ceramides can modulate secretion and endocytic recycling functions of the redundant v-SNAREs Snc1 and Snc2, because addition of exogenous PHS to the growth medium could restore Golgi to plasma membrane transport in yeast mutants defective for Snc1/2 and the t-SNAREs Sso1/2 (41). In addition, the growth defect of *snc1*Δ *snc2*Δ mutant can also be suppressed by altering the availability of different ceramide precursors (14, 43). How alterations in sphingolipids suppress the sorting defects of the *snc1*Δ *snc2*Δ mutant is unclear, but

could be due to changes in sphingolipid signaling or membrane curvature and fluidity. Perhaps in support of a signaling mechanism, we found that the Can1 transport defect is phenocopied by a yeast mutant defective in Pkh function suggesting that Pkh kinases and Slm proteins affect Can1 trafficking by a common mechanism. The role of Slm proteins and Pkh1/2 kinases in Can1 plasma membrane delivery may be dependent on their roles in regulating actin cytoskeletal polarization, because intracellular retention of Can1 is also observed upon disruption of actin filaments by latrunculin A. While the precise mechanism by which Slm proteins affects Can1 transport remains to be determined, our studies suggest that Slm proteins act downstream of an sphingolipid-derived signal to control the organization of the actin cytoskeleton in response to heat stress. Thus, Slm proteins are subject to control by multiple signaling pathways, including $PI(4,5)P_2$ TorC2 and sphingolipid-activated Pkh kinases, and it will be interesting to determine whether and how input of these different signals is integrated to temporally and spatially affect actin organization.

Note added in proof:

While this manuscript was under review, two other papers were published (8, 54) reporting on a role of Slm proteins in sphingolipid metabolism(54), the regulation of calcineurin activity (54), as well as the modulation of Slm phosphorylation by sphingolipids and calcineurin (8). Our data demonstrating antagonistic roles of sphingolipids and calcineurin in the modulation of Slm phosphorylation are in good agreement with studies by Bultynck et al. (8). In addition, a role of Slm proteins in the maintenance of normal cellular sphingolipid levels and downregulation of calcineurin activity, as reported by Tabuchi et al. (54), may explain, in part, the Can1 trafficking and actin defects observed in *slm* mutants.

ACKNOWLEDGMENTS

We thank Sandra K. Lemmon, Kunihiro Matsumoto, Widmar Tanner, and Jeremy Thorner for their generous gifts of strains and plasmids, Eric Chang for the gift of canavanine and latrunculin A, and Felicity Ashcroft for comments on the manuscript. This work was supported by grants GM068098 and GM068098-S1 from the National Institutes of Health, and grant 0555128Y from the American Heart Association. This manuscript is dedicated to the memory of Sarah Leigh Rodgerson.

REFERENCES

1. **Audhya, A., and S. D. Emr.** 2002. Stt4 PI 4-kinase localizes to the plasma membrane and functions in the Pkc1-mediated MAP kinase cascade. Dev Cell **2:**593-605.

2. **Audhya, A., M. Foti, and S. D. Emr.** 2000. Distinct roles for the yeast phosphatidylinositol 4-kinases, Stt4p and Pik1p, in secretion, cell growth, and organelle membrane dynamics. Mol Biol Cell **11:**2673-89.

3. **Audhya, A., R. Loewith, A. B. Parsons, L. Gao, M. Tabuchi, H. Zhou, C. Boone, M. N. Hall, and S. D. Emr.** 2004. Genome-wide lethality screen identifies new PI4,5P(2) effectors that regulate the actin cytoskeleton. Embo J **23:**3747-57.

4. **Bagnat, M., S. Keranen, A. Shevchenko, and K. Simons.** 2000. Lipid rafts function in biosynthetic delivery of proteins to the cell surface in yeast. Proc Natl Acad Sci U S A **97:**3254-9.

5. **Beeler, T., D. Bacikova, K. Gable, L. Hopkins, C. Johnson, H. Slife, and T. Dunn.** 1998. The Saccharomyces cerevisiae TSC10/YBR265w gene encoding 3-ketosphinganine reductase is identified in a screen for temperature-sensitive suppressors of the Ca2+-sensitive csg2Delta mutant. J Biol Chem **273:**30688-94.

6. **Beeler, T. J., D. Fu, J. Rivera, E. Monaghan, K. Gable, and T. M. Dunn.** 1997. SUR1 (CSG1/BCL21), a gene necessary for growth of Saccharomyces cerevisiae in the presence of high Ca2+ concentrations at 37 degrees C, is required for mannosylation of inositolphosphorylceramide. Mol Gen Genet **255:**570-9.

7. **Birchwood, C. J., J. D. Saba, R. C. Dickson, and K. W. Cunningham.** 2001. Calcium influx and signaling in yeast stimulated by intracellular sphingosine 1-phosphate accumulation. J Biol Chem **276:**11712-8.

8. **Bultynck, G., V. L. Heath, A. P. Majeed, J. M. Galan, R. Haguenauer-Tsapis, and M. S. Cyert.** 2006. Slm1 and slm2 are novel substrates of the calcineurin phosphatase required for heat stress-induced endocytosis of the yeast uracil permease. Mol Cell Biol **26:**4729-45.

9. **Casamayor, A., P. D. Torrance, T. Kobayashi, J. Thorner, and D. R. Alessi.** 1999. Functional counterparts of mammalian protein kinases PDK1 and SGK in budding yeast. Curr Biol **9:**186-97.

10. **Chung, N., G. Jenkins, Y. A. Hannun, J. Heitman, and L. M. Obeid.** 2000. Sphingolipids signal heat stress-induced ubiquitin-dependent proteolysis. J Biol Chem **275:**17229-32.

11. **Cowart, L. A., Y. Okamoto, F. R. Pinto, J. L. Gandy, J. S. Almeida, and Y. A. Hannun.** 2003. Roles for sphingolipid biosynthesis in mediation of specific programs of the heat stress response determined through gene expression profiling. J Biol Chem **278:**30328-38.

12. **Cyert, M. S.** 2003. Calcineurin signaling in Saccharomyces cerevisiae: how yeast go crazy in response to stress. Biochem Biophys Res Commun **311:**1143-50.

13. **Cyert, M. S., R. Kunisawa, D. Kaim, and J. Thorner.** 1991. Yeast has homologs (CNA1 and CNA2 gene products) of mammalian calcineurin, a calmodulin-regulated phosphoprotein phosphatase. Proc Natl Acad Sci U S A **88:**7376-80.

14. **David, D., S. Sundarababu, and J. E. Gerst.** 1998. Involvement of long chain fatty acid elongation in the trafficking of secretory vesicles in yeast. J Cell Biol **143:**1167-82.

15. **Desrivieres, S., F. T. Cooke, H. Morales-Johansson, P. J. Parker, and M. N. Hall.** 2002. Calmodulin controls organization of the actin cytoskeleton via regulation of

phosphatidylinositol (4,5)-bisphosphate synthesis in Saccharomyces cerevisiae. Biochem J **366:**945-51.

16. **Desrivieres, S., F. T. Cooke, P. J. Parker, and M. N. Hall.** 1998. MSS4, a phosphatidylinositol-4-phosphate 5-kinase required for organization of the actin cytoskeleton in Saccharomyces cerevisiae. J Biol Chem **273:**15787-93.

17. **Dickson, R. C.** 1998. Sphingolipid functions in Saccharomyces cerevisiae: comparison to mammals. Annu Rev Biochem **67:**27-48.

18. **Dickson, R. C., and R. L. Lester.** 2002. Sphingolipid functions in Saccharomyces cerevisiae. Biochim Biophys Acta **1583:**13-25.

19. **Dickson, R. C., E. E. Nagiec, M. Skrzypek, P. Tillman, G. B. Wells, and R. L. Lester.** 1997. Sphingolipids are potential heat stress signals in Saccharomyces. J Biol Chem **272:**30196-200.

20. **Fadri, M., A. Daquinag, S. Wang, T. Xue, and J. Kunz.** 2005. The pleckstrin homology domain proteins Slm1 and Slm2 are required for actin cytoskeleton organization in yeast and bind phosphatidylinositol-4,5-bisphosphate and TORC2. Mol Biol Cell **16:**1883-900.

21. **Ferguson-Yankey, S. R., M. S. Skrzypek, R. L. Lester, and R. C. Dickson.** 2002. Mutant analysis reveals complex regulation of sphingolipid long chain base phosphates and long chain bases during heat stress in yeast. Yeast **19:**573-86.

22. **Friant, S., R. Lombardi, T. Schmelzle, M. N. Hall, and H. Riezman.** 2001. Sphingoid base signaling via Pkh kinases is required for endocytosis in yeast. Embo J **20:**6783-92.

23. **Friant, S., B. Zanolari, and H. Riezman.** 2000. Increased protein kinase or decreased PP2A activity bypasses sphingoid base requirement in endocytosis. Embo J **19:**2834-44.

24. **Futerman, A. H., and Y. A. Hannun.** 2004. The complex life of simple sphingolipids. EMBO Rep **5:**777-82.

25. **Gould, K. L., L. Ren, A. S. Feoktistova, J. L. Jennings, and A. J. Link.** 2004. Tandem affinity purification and identification of protein complex components. Methods **33:**239-44.

26. **Hearn, J. D., R. L. Lester, and R. C. Dickson.** 2003. The uracil transporter Fur4p associates with lipid rafts. J Biol Chem **278:**3679-86.

27. **Ho, H. L., Y. S. Shiau, and M. Y. Chen.** 2005. SaccharomycesTSC11/AVO3 participates in regulating cell integrity and functionally interacts with components of the Tor2 complex. Curr Genet **47:**273-88.

28. **Homma, K., S. Terui, M. Minemura, H. Qadota, Y. Anraku, Y. Kanaho, and Y. Ohya.** 1998. Phosphatidylinositol-4-phosphate 5-kinase localized on the plasma membrane is essential for yeast cell morphogenesis. J Biol Chem **273:**15779-86.

29. **Inagaki, M., T. Schmelzle, K. Yamaguchi, K. Irie, M. N. Hall, and K. Matsumoto.** 1999. PDK1 homologs activate the Pkc1-mitogen-activated protein kinase pathway in yeast. Mol Cell Biol **19:**8344-52.

30. **Ito, H., Y. Fukuda, K. Murata, and A. Kimura.** 1983. Transformation of intact yeast cells treated with alkali cations. J Bacteriol **153:**163-8.

31. **Ito, T., T. Chiba, R. Ozawa, M. Yoshida, M. Hattori, and Y. Sakaki.** 2001. A comprehensive two-hybrid analysis to explore the yeast protein interactome. Proc Natl Acad Sci U S A **98:**4569-74.

32. **Jenkins, G. M., A. Richards, T. Wahl, C. Mao, L. Obeid, and Y. Hannun.** 1997. Involvement of yeast sphingolipids in the heat stress response of Saccharomyces cerevisiae. J Biol Chem **272:**32566-72.

33. **Jung, S. Y., A. Malovannaya, J. Wei, B. W. O'Malley, and J. Qin.** 2005. Proteomic analysis of steady-state nuclear hormone receptor coactivator complexes. Mol Endocrinol **19:**2451-65.

34. **Kobayashi, T., H. Takematsu, T. Yamaji, S. Hiramoto, and Y. Kozutsumi.** 2005. Disturbance of sphingolipid biosynthesis abrogates the signaling of Mss4, phosphatidylinositol-4-phosphate 5-kinase, in yeast. J Biol Chem **280:**18087-94.

35. **Lee, M. C., S. Hamamoto, and R. Schekman.** 2002. Ceramide biosynthesis is required for the formation of the oligomeric H+-ATPase Pma1p in the yeast endoplasmic reticulum. J Biol Chem **277:**22395-401.

36. **Liu, J.** 1993. FK506 and cyclosporin, molecular probes for studying intracellular signal transduction. Immunol Today **14:**290-5.

37. **Liu, K., X. Zhang, R. L. Lester, and R. C. Dickson.** 2005. The sphingoid long chain base phytosphingosine activates AGC-type protein kinases in Saccharomyces cerevisiae including Ypk1, Ypk2, and Sch9. J Biol Chem **280:**22679-87.

38. **Luo, C., K. T. Shaw, A. Raghavan, J. Aramburu, F. Garcia-Cozar, B. A. Perrino, P. G. Hogan, and A. Rao.** 1996. Interaction of calcineurin with a domain of the transcription factor NFAT1 that controls nuclear import. Proc Natl Acad Sci U S A **93:**8907-12.

39. **Malinska, K., J. Malinsky, M. Opekarova, and W. Tanner.** 2004. Distribution of Can1p into stable domains reflects lateral protein segregation within the plasma membrane of living S. cerevisiae cells. J Cell Sci **117:**6031-41.

40. **Malinska, K., J. Malinsky, M. Opekarova, and W. Tanner.** 2003. Visualization of protein compartmentation within the plasma membrane of living yeast cells. Mol Biol Cell **14:**4427-36.

41. **Marash, M., and J. E. Gerst.** 2001. t-SNARE dephosphorylation promotes SNARE assembly and exocytosis in yeast. Embo J **20:**411-21.

42. **Nagiec, M. M., M. Skrzypek, E. E. Nagiec, R. L. Lester, and R. C. Dickson.** 1998. The LCB4 (YOR171c) and LCB5 (YLR260w) genes of Saccharomyces encode sphingoid long chain base kinases. J Biol Chem **273:**19437-42.

43. **Oh, C. S., D. A. Toke, S. Mandala, and C. E. Martin.** 1997. ELO2 and ELO3, homologues of the Saccharomyces cerevisiae ELO1 gene, function in fatty acid elongation and are required for sphingolipid formation. J Biol Chem **272:**17376-84.

44. **Ono, B. I., Y. Ishino, and S. Shinoda.** 1983. Nonsense mutations in the can1 locus of Saccharomyces cerevisiae. J Bacteriol **154:**1476-9.

45. **Opekarova, M., K. Malinska, L. Novakova, and W. Tanner.** 2005. Differential effect of phosphatidylethanolamine depletion on raft proteins: further evidence for diversity of rafts in Saccharomyces cerevisiae. Biochim Biophys Acta **1711:**87-95.

46. **Roelants, F. M., P. D. Torrance, N. Bezman, and J. Thorner.** 2002. Pkh1 and pkh2 differentially phosphorylate and activate ypk1 and ykr2 and define protein kinase modules required for maintenance of cell wall integrity. Mol Biol Cell **13:**3005-28.

47. **Roelants, F. M., P. D. Torrance, and J. Thorner.** 2004. Differential roles of PDK1- and PDK2-phosphorylation sites in the yeast AGC kinases Ypk1, Pkc1 and Sch9. Microbiology **150:**3289-304.

48. **Schmidt, A., J. Kunz, and M. N. Hall.** 1996. TOR2 is required for organization of the actin cytoskeleton in yeast. Proc Natl Acad Sci U S A **93:**13780-5.

49. **Sherman, F., G. R. Fink, and J. B. Hicks.** 1983. Methods in Yeast Genetics. Cold Spring Harbor Laboratory Press, Cold Spring Harbor, NY.

50. **Simons, K., and E. Ikonen.** 1997. Functional rafts in cell membranes. Nature **387:**569-72.

51. **Skrzypek, M., R. L. Lester, and R. C. Dickson.** 1997. Suppressor gene analysis reveals an essential role for sphingolipids in transport of glycosylphosphatidylinositol-anchored proteins in Saccharomyces cerevisiae. J Bacteriol **179:**1513-20.

52. **Skrzypek, M. S., M. M. Nagiec, R. L. Lester, and R. C. Dickson.** 1999. Analysis of phosphorylated sphingolipid long-chain bases reveals potential roles in heat stress and growth control in Saccharomyces. J Bacteriol **181:**1134-40.

53. **Sun, Y., R. Taniguchi, D. Tanoue, T. Yamaji, H. Takematsu, K. Mori, T. Fujita, T. Kawasaki, and Y. Kozutsumi.** 2000. Sli2 (Ypk1), a homologue of mammalian protein kinase SGK, is a downstream kinase in the sphingolipid-mediated signaling pathway of yeast. Mol Cell Biol **20:**4411-9.

54. **Tabuchi, M., A. Audhya, A. B. Parsons, C. Boone, and S. D. Emr.** 2006. The phosphatidylinositol 4,5-biphosphate and TORC2 binding proteins Slm1 and Slm2 function in sphingolipid regulation. Mol Cell Biol **26:**5861-75.

55. **Takenawa, T., and T. Itoh.** 2001. Phosphoinositides, key molecules for regulation of actin cytoskeletal organization and membrane traffic from the plasma membrane. Biochim Biophys Acta **1533:**190-206.

56. **Uemura, S., A. Kihara, J. Inokuchi, and Y. Igarashi.** 2003. Csg1p and newly identified Csh1p function in mannosylinositol phosphorylceramide synthesis by interacting with Csg2p. J Biol Chem **278:**45049-55.

57. **Uetz, P., L. Giot, G. Cagney, T. A. Mansfield, R. S. Judson, J. R. Knight, D. Lockshon, V. Narayan, M. Srinivasan, P. Pochart, A. Qureshi-Emili, Y. Li, B. Godwin, D. Conover, T. Kalbfleisch, G. Vijayadamodar, M. Yang, M. Johnston, S. Fields, and J. M. Rothberg.** 2000. A comprehensive analysis of protein-protein interactions in Saccharomyces cerevisiae. Nature **403:**623-7.

58. **Wells, G. B., R. C. Dickson, and R. L. Lester.** 1998. Heat-induced elevation of ceramide in Saccharomyces cerevisiae via de novo synthesis. J Biol Chem **273:**7235-43.

59. **Yin, H. L., and P. A. Janmey.** 2003. Phosphoinositide regulation of the actin cytoskeleton. Annu Rev Physiol **65:**761-89.

60. **Zanolari, B., S. Friant, K. Funato, C. Sutterlin, B. J. Stevenson, and H. Riezman.** 2000. Sphingoid base synthesis requirement for endocytosis in Saccharomyces cerevisiae. Embo J **19:**2824-33.

61. **Zhao, C., T. Beeler, and T. Dunn.** 1994. Suppressors of the Ca(2+)-sensitive yeast mutant (csg2) identify genes involved in sphingolipid biosynthesis. Cloning and characterization of SCS1, a gene required for serine palmitoyltransferase activity. J Biol Chem **269:**21480-8.

FIGURE LEGENDS

Figure 1. Pathways involved in sphingolipid biosynthesis in *S. cerevisiae*. A schematic overview of the sphingolipid biosynthetic and degradation pathways is shown. Steps in sphingolipid biosynthesis blocked by chemical inhibitors myriocin and aureobasidin A are indicated. Deletion mutants used to test for genetic interactions with the *slm1*Δ mutant are boxed.

Figure 2. Deletion of *SLM1* confers supersensitivity to myriocin. (A) Isogenic wild type, *slm1*Δ, and *slm2*Δ mutant strains were grown to stationary phase in YPD medium and serial dilutions of cultures were spotted on YPD plates containing either drug vehicle alone or the indicated concentrations of myriocin. (B) Addition of exogenous PHS (10 μM) to YPD plates containing 0.5 μg/ml myriocin rescues growth of the *slm1*Δ mutant. All plates were incubated at 30˚C and photographed after 3 days.

Figure 3. Synthetic genetic interactions between *slm1*Δ and mutants in the sphingolipid biosynthesis pathway.

(A) Serial dilutions of isogenic wild type, *slm1*Δ, *csg2*Δ, *fen1*Δ, and *lcb4*Δ single mutant and *slm1*Δ *csg2*Δ, *slm1*Δ *fen1*Δ, and *slm1*Δ *lcb4*Δ double mutant yeast cultures were spotted on YPD plates. Plates were incubated at 26˚C and 38˚C and photographed after 3 days. (B) Exponentially growing wild type, *slm1*Δ, *csg2*Δ, *fen1*Δ, and *lcb4*Δ single mutant and *slm1*Δ *csg2*Δ, *slm1*Δ *fen1*Δ, and *slm1*Δ *lcb4*Δ double mutant yeast cultures grown at 26°C were shifted to 38˚C for 2 h. Cells were fixed and stained with Alexa594-phalloidin to visualize the actin cytoskeleton. (C) Small to medium budded cells from (B) were scored for their actin polarization state. Cells were

classified as having a polarized (containing cables and polarized actin patches), partially polarized (containing cables and partially polarized patches) or depolarized actin cytoskeleton (containing no cables and depolarized patches). 100 cells per sample were counted.

Figure 4. Slm1 and Slm2 phosphorylation in response to heat stress is dependent on sphingolipid synthesis.

Western blot analysis of phosphorylated Slm1 (A) and Slm2 (B) proteins. Cells expressing Slm1-TAP and Slm2-TAP were grown to mid-logarithmic phase in YPD medium at 26˚C, aliquots of cells were then treated with vehicle alone (DMSO), myriocin (2 μg/ml) or exogenous PHS (10 μM) for 30 min at RT, and heat shocked shifted to 38^{o}C for the indicated times. Cell extracts were prepared and subjected to TAP purification using IgG-sepharose beads. Bound proteins were eluted with SDS-PAGE buffer, separated by SDS–PAGE and immunoblotted with antibodies directed against phosphoserine (Q5) and phosphothreonine (Q7). Note that Slm2 Western blots were exposed to ECL reagents eight times longer than Slm1. (C) Quantitation of kinetics of Slm1 and Slm2 phosphorylation in response to heat stress in the presence or absence of drugs. Densitometric measurements of Western blots in (A) and (B) were determined using Image Gauge 4.0 program. The extent of Q5 and Q7 signals were normalized to the TAP signal for each indicated time point. Results from two independent experiments are shown.

Figure 5. The $Ca^{2+/}$calmodulin-dependent protein phosphatase calcineurin dephosphorylates Slm1.

(A) Sequence alignment of Slm1 and Slm2 with known calcineurin binding sites. The consensus calcineurin-binding motif is indicated below the sequence alignment. (B) *In vitro* transcribed and

translated [^{35}S]-labeled Cna1 was incubated with beads alone or with beads containing bound recombinant 6His-Slm1 or 6His-Slm2 proteins or Slm mutant variants lacking the calcineurin binding motif. Bound [^{35}S]-labeled proteins that remained after washing were analyzed by SDS-PAGE and autoradiography. The molecular weights of protein markers are indicated to the left. (C) Cells expressing Slm1-TAP were grown to mid-logarithmic phase in YPD medium at 26˚C, cells were then divided into aliquots and treated for 30 min at RT with vehicle alone (DMSO), 100 mM $CaCl_2$, 1,2-*bis*(*o*-aminophenoxy)ethane-*N,N,N',N'*-tetraacetic acid (BAPTA; 10 μM) or FK506 (2 μg/ml). Cells were shifted to 38^{o}C for the indicated times and cell extracts were prepared and subjected to TAP purification using IgG-sepharose beads. Bound proteins were separated by SDS–PAGE and immunoblotted with antibodies directed against phosphoserine (Q5) and phosphothreonine (Q7). (D) Densitometric analysis of phosphorylation levels of Slm1-TAP from (C). Western blots were digitized using Image Gauge 4.0 program and the levels of phosphorylation were normalized to the TAP signal in each time point. (E) Wild type cells expressing Slm1-TAP or the Slm1$_{\Delta CN}$-TAP mutant from a low-copy vector under control of the Gal1 promoter were grown at 26 ˚C in the presence of galactose for 2 1/2 hr to induce expression of the TAP fusion protein. Glucose was then added to shut off expression and incubation was continued for 30 min at 26˚C. Cells were then heat shocked at 38^{o}C for the indicated times. Extracts were prepared and analyzed as described in (C). (F) Densitometric analysis of phosphorylation levels of Slm1-TAP from (E). Results from two independent experiments are shown.

Figure 6. FK506 and exogenous PHS rescue the lethality of *slm1-ts slm2*Δ mutant cells. Serial dilutions of isogenic wild type, and *slm1-ts slm2*Δ mutant yeast cultures were spotted on

YPD plates containing either drug vehicle (Tween-20/EtOH; Control) or supplemented with FK506 (2 μg/ml), and PHS (10 μM) alone, or in combination. Plates were incubated at 37˚C and photographed after 3 days.

Figure 7. Slm1 phosphorylation is dependent on the sphingolipid-activated kinases Pkh1/2 and Pkh2, but is independent of Ypk1/2 and Tor2. (A) Exponentially growing wild-type or temperature-sensitive *pkh1*^{ts}Δ*pkh2* mutant cells that contain HA-Slm1 under the control of a galactose-inducible promoter were grown at 26 ˚C in the presence of galactose for 2 1/2 hr to induce expression of HA-Slm1. Glucose was then added to shut off expression and incubation was continued for 30 min at 26˚C. Cells were then heat shocked at 38^{o}C for the indicated times. Extracts were prepared and subjected to affinity purification on anti-HA-sepharose beads. Bound proteins were separated by SDS–PAGE and immunoblotted with antibodies directed against phosphoserine (Q5), phosphothreonine (Q7), and HA. (B) Western blot analysis of phosphorylated HA-Slm1 expressed in temperature-sensitive *ypk1-ts ypk2*Δ mutant cells (strain YPT40) is shown. HA-Slm1 was expressed and analyzed as described in (A). (C) Western blot analysis of phosphorylated HA-Slm1 expressed in temperature-sensitive *tor1*Δ *tor2-ts* cells (strain SH121) is shown. HA-Slm1 was expressed and analyzed as described in (A). (D) Western blot densitometric analysis of phosphorylation levels of HA-Slm1. Blots were digitized using Image Gauge 4.0 program and the levels of phosphorylation were normalized to the HA signal.

Figure 8. Mutation of Ser659 abrogates Slm1 phosphorylation and Slm1-dependent survival under heat stress conditions. (A) Cells expressing HA-tagged Slm1$_{S659A}$ under control of the *GAL1* promoter were grown at 26 ˚C in the presence of galactose for 2 1/2 hr to induce

expression of HA-Slm1. Glucose was then added to shut off expression and incubation was continued for 30 min at 26˚C. Cells were then heat shocked at 38˚C for the indicated times. Extracts were prepared and subjected to affinity purification on anti-HA-sepharose beads. Bound proteins were separated by SDS–PAGE and immunoblotted with antibodies directed against phosphoserine (Q5), phosphothreonine (Q7), and HA. (B) Densitometric analysis of phosphorylation levels of HA-Slm1$_{S659A}$ from (A). (C) Growth of strain JK520 transformed with *LEU2* plasmids containing either wild type *SLM1* or the *SLM1*$_{S659A}$ and *SLM1*$_{\Delta C}$ mutant variants at 30˚C and 38˚C is shown on medium containing 5-fluoroorotic acid (+5-FOA), which counterselects the *SLM1 URA3* plasmid.

Figure 9. *SLM1* overexpression partially corrects growth and actin polarization defects of *pkh1-ts pkh2*Δ mutant cells. (A) Vector alone or plasmids containing *PKH1, SLM1, SLM1*$_{S659D,}$ *or SLM1*$_{\Delta CN}$, under the control of the galactose-inducible *GAL1* promoter, were transformed into the temperature sensitive *pkh1-ts pkh2*Δ mutant strain. Growth of transformants was tested on synthetic complete medium containing galactose as carbon source and supplemented with 1 M sorbitol (SG-Sorb). Plates were incubated at the indicated temperatures and photographed after 3-4 days. (B) *pkh1-ts pkh2*Δ cells containing the indicated plasmids were grown at 26˚C in medium supplemented with 1 M sorbitol and galactose. Cells were then shifted to 38˚C for 2hr, fixed and the actin cytoskeleton was visualized with Alexa594-phalloidin. (C) Small to medium budded *pkh1-ts pkh2*Δ mutants cells transformed with the indicated plasmids from (B) were scored for their actin polarization state. Cells were classified as having a polarized (containing cables and polarized actin patches), partially polarized (containing cables and partially polarized patches) or depolarized actin cytoskeleton (containing no cables and depolarized patches). 150

cells per sample were counted.

Figure 10. Loss of Slm function results in defective delivery of the arginine transporter Can1 to the plasma membrane.

(A) A plasmid encoding for Can1p-GFP was expressed in wt (W303), *slm1-ts slm2*Δ, *pkh1-ts pkh2*Δ*, erg24*Δ, and *lcb1-100* strains and Can1-GFP was visualized in living cells grown at the permissive (26˚C) or nonpermissive (38˚C) temperature for 1 hr. Representative examples of GFP localization are shown. GFP signal is shown in the top panels, DIC images of the same cells are shown in the bottom panels. (B) Can1-GFP localization is shown in *slm1-ts slm2*Δ mutant cells (strain JK515) containing empty vector (left and right panels) or *SLM1* expressed from a high-copy vector under the control of the GPD promoter (*2μ*, *TRP1*; middle panel). Cells were either left untreated or were incubated in the presence of PHS (7.5 μM) and FK506 (2 μg/ml) for 1 hr at 26˚C before being shifted to 38˚C for 2 hr and GFP fluorescence was visualized. (C) Can1-GFP localization is shown in *pkh1-ts pkh2*Δ mutant cells containing empty vector (left panel) or *SLM1* expressed from a high-copy vector under the control of the GPD promoter (*2μ*, *TRP1*; right panel). Vector-transformed cells were left untreated, whereas cells expressing *SLM1* were incubated in the presence of FK506 (2 μg/ml) for 1 hr at 26˚C before being shifted to 38˚C for 2 hr and GFP fluorescence was visualized. (D) Serial dilutions of wild type (W303), *lcb1-100*, and *slm1-ts slm2*Δ (JK515) strains transformed with empty vector or p*CAN1-GFP* were plated on media lacking Arg to verify plating (left panel) and on medium lacking Arg and containing the arginine analog canavanine (0.5 μg/ml). Plates were incubated at 30°C for 3 days. (E). Wild type cells (W303) containing a plasmid encoding for Can1p-GFP were treated with

latrunculin A (5 μM) at 30˚C and GFP fluorescence was recorded in living cells at the indicated times.

Supplementary Figure 1. Extent of Slm1 co-localization with lipid raft microdomain markers Pma1, Can1, and Sur7. A) To determine the extent of co-localization of Slm1 with Pma1 and Can1/Sur7, which were reported to localize to distinct lipid raft microdomains (40), cells containing chromosomally expressed Pma1-GFP, Can1-GFP, and Sur7-GFP fusion proteins were transformed with a low-copy plasmid containing *HA-SLM1* under control of the *GAL1* promoter. Transformed cells were grown to exponential phase in S-raffinose medium at 30˚C and expression of *HA-SLM1* was induced by addition of galactose to the growth medium for 90 min. Cells were then fixed and HA-Slm1 was visualized by indirect immunofluorescence using mouse monoclonal anti-HA antibody followed by Cy3-conjugated goat anti-mouse IgG. GFP fusion proteins were visualized with a rabbit polyclonal anti-GFP antiserum followed by Cy2-conjugated goat anti-rabbit IgG. B) Cells containing chromosomally expressed Can1-GFP were grown as in A), fixed and endogenous Pma1 was visualized using mouse monoclonal anti-Pma1 antibody followed by Cy3-conjugated goat anti-mouse IgG. GFP fusion protein was visualized with a rabbit polyclonal anti-GFP antiserum followed by Cy2-conjugated goat anti-rabbit IgG.

Supplementary Figure 2. FK506 and PHS suppress synthetic genetic interactions between *slm1*Δ and mutants in the sphingolipid biosynthesis pathway.

(A) Serial dilutions of isogenic wild type, *slm1*Δ, *csg2*Δ, *fen1*Δ, and *lcb4*Δ single mutant and *slm1*Δ *csg2*Δ, *slm1*Δ *fen1*Δ, and *slm1*Δ *lcb4*Δ double mutant yeast cultures were spotted on YPD plates containing PHS (5 μg/ml), FK506 (2 μg/ml), or the combination of PHS and FK506.

Table I. *Saccharomyces cerevisiae* strains used in this study

Strain	Genotype	Source
W303a	*MATa ade2-1 trp1-1 can1-100 leu2-3,112 his3-11,15 ura3-1 GAL+*	Lab collection
W303α	*MATa ade2-1 trp1-1 can1-100 leu2-3,112 his3-11,15 ura3-1 GAL+*	Lab collection
BY4741	MATa; his3Δ1; leu2Δ0; met15Δ0; ura3Δ0	Lab collection
95700	BY4741 except *SLM1-GFP-URA3*	Research Genetics
7502123	BY4741 except *SLM1-TAP-HIS3*	Open Biosystems
7501161	BY4741 except *SLM2-TAP-HIS3*	Open Biosystems
RH3804	MATα *lcb1–100 trp1 leu2 ura3 lys2 bar1*	H. Riezman, University of Geneva, Switzerland
*erg24*Δ	BY4741 except *erg24:: KanMX*	(38)
JK502	W303a except *slm1::KanMX*	(19)
JK506	W303a except *slm2::HIS3*	(19)
JK515	W303a except *slm1::KanMX slm2::HIS3* carrying p*416GPD-slm1-3*	This study
JK520	W303a except *slm1::KanMX slm2::HIS3* /pAS25::*SLM1*	This study
ypc1Δ	W303α except *ypc1:: KanMX TRP1*	This study
*sur1*Δ	W303α except *sur1:: KanMX TRP1*	This study
*lcb3*Δ	W303α except *lcb3:: KanMX TRP1*	This study

*lcb4*Δ	W303α except *lcb4:: KanMX TRP1*	This study
*fen1*Δ	W303α except *fen1:: KanMX TRP1*	This study
*csg2*Δ	W303α except *csg2:: KanMX*	This study
*ipt1*Δ	W303α except *ipt1:: KanMX*	This study
*pkh1-ts pkh2*Δ	*pkh1-D398G pkh2::LEU2*	(28)
YPT40	*MAT***a** *ypk1-1^{ts}:HIS3 ypk2::TRP1 ade2-101 his3-200 leu2-1 lys2-801 trp1-1 ura3-52*	(8)
SH121	JK9-3d**a** *ade2/ tor2::ADE2*/YCplac111::*tor2*-21	M. Hall

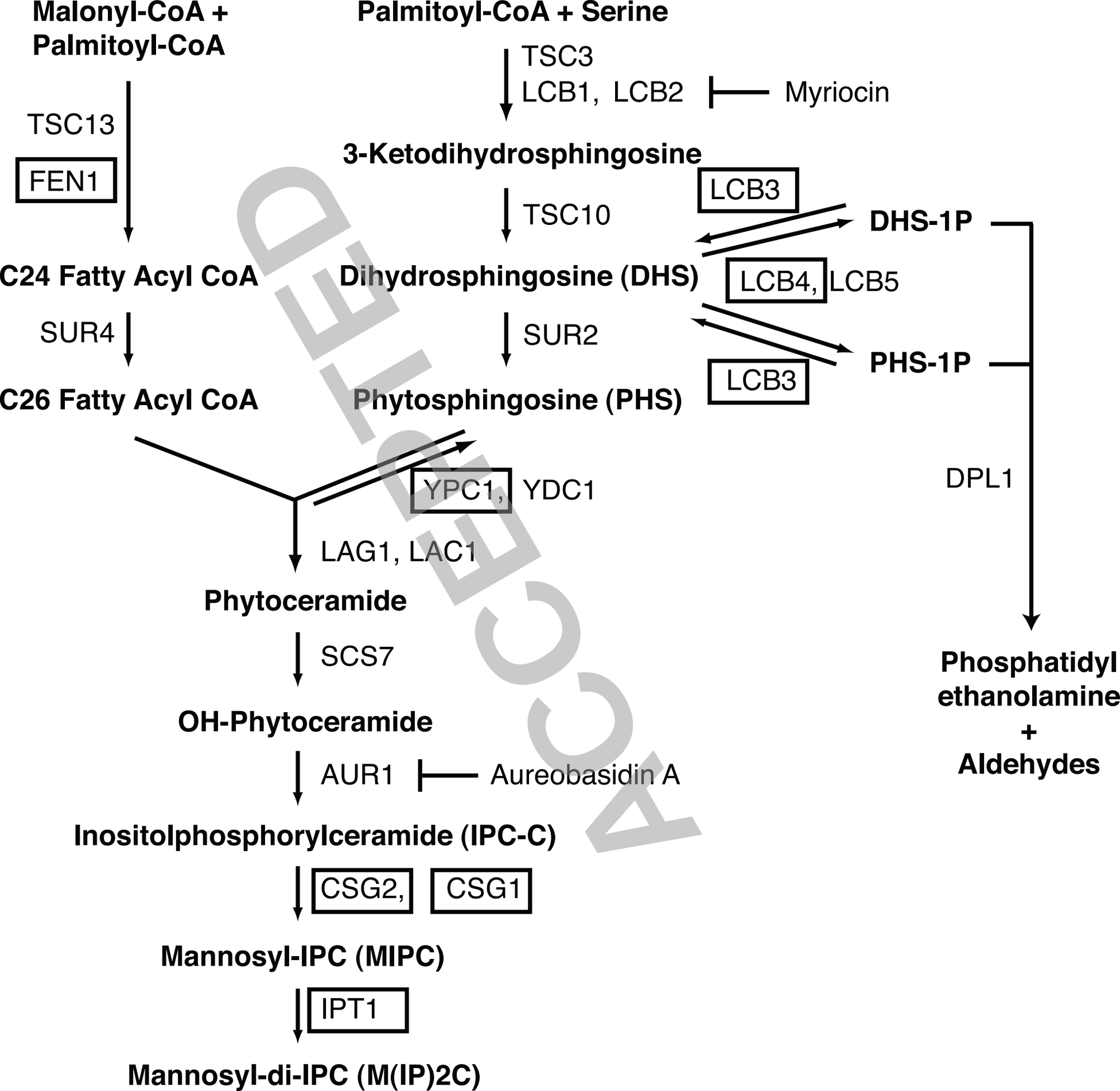
Malonyl-CoA +
Palmitoyl-CoA
Palmitoyl-CoA + Serine
TSC3
LCB1, LCB2
Myriocin
TSC13
FEN1
3-Ketodihydrosphingosine
LCB3
TSC10
DHS-1P
C24 Fatty Acyl CoA
Dihydrosphingosine (DHS)
LCB4, LCB5
SUR4
SUR2
PHS-1P
LCB3
C26 Fatty Acyl CoA
Phytosphingosine (PHS)
DPL1
YPC1, YDC1
LAG1, LAC1
Phytoceramide
SCS7
OH-Phytoceramide
AUR1
Aureobasidin A
Phosphatidyl
ethanolamine
+
Aldehydes
Inositolphosphorylceramide (IPC-C)
CSG2, CSG1
Mannosyl-IPC (MIPC)
IPT1
Mannosyl-di-IPC (M(IP)2C)

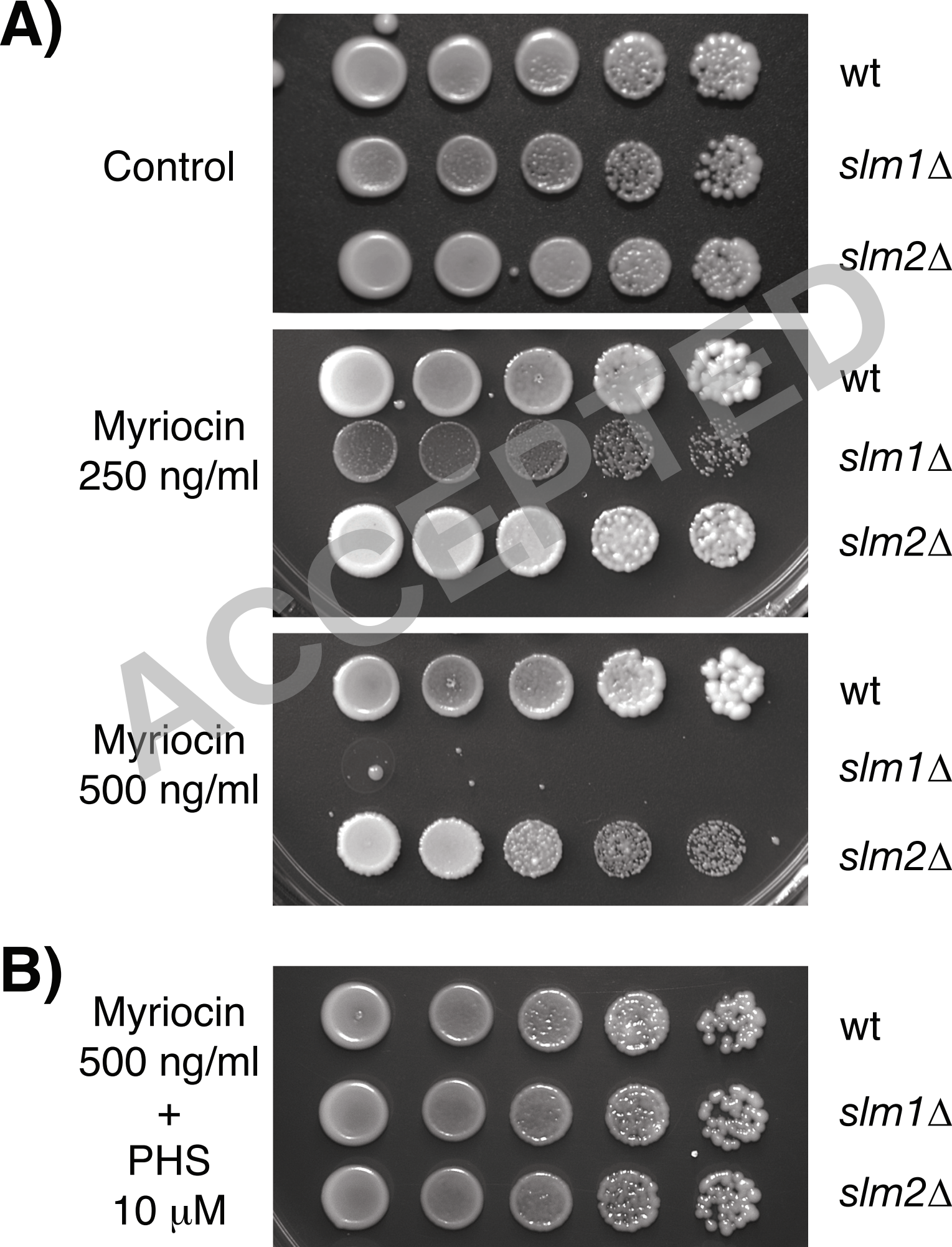
A)
Control
wt
slm1Δ
slm2Δ
Myriocin
250 ng/ml
wt
slm1Δ
slm2Δ
Myriocin
500 ng/ml
wt
slm1Δ
slm2Δ
B)
Myriocin
500 ng/ml
+
PHS
10 μM
wt
slm1Δ
slm2Δ

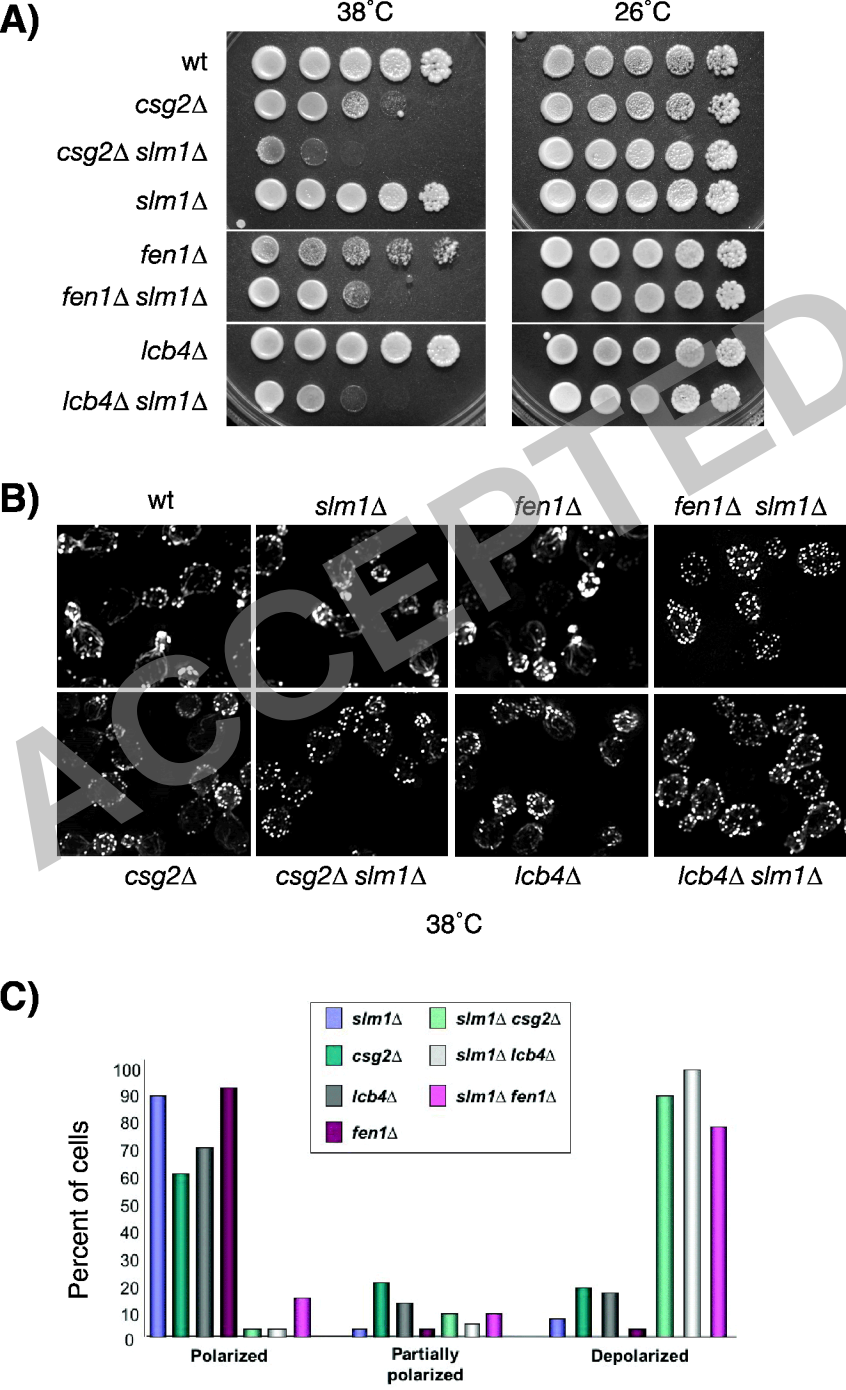
A)
38˚C
26˚C
wt
csg2Δ
csg2Δ slm1Δ
slm1Δ
fen1Δ
fen1Δ slm1Δ
lcb4Δ
lcb4Δ slm1Δ
B)
wt
slm1Δ
fen1Δ
fen1Δ slm1Δ
csg2Δ
csg2Δ slm1Δ
lcb4Δ
lcb4Δ slm1Δ
38˚C
C)
slm1Δ
csg2Δ
lcb4Δ
fen1Δ
slm1Δ csg2Δ
slm1Δ lcb4Δ
slm1Δ fen1Δ
Percent of cells
100
90
80
70
60
50
40
30
20
10
0
Polarized
Partially polarized
Depolarized

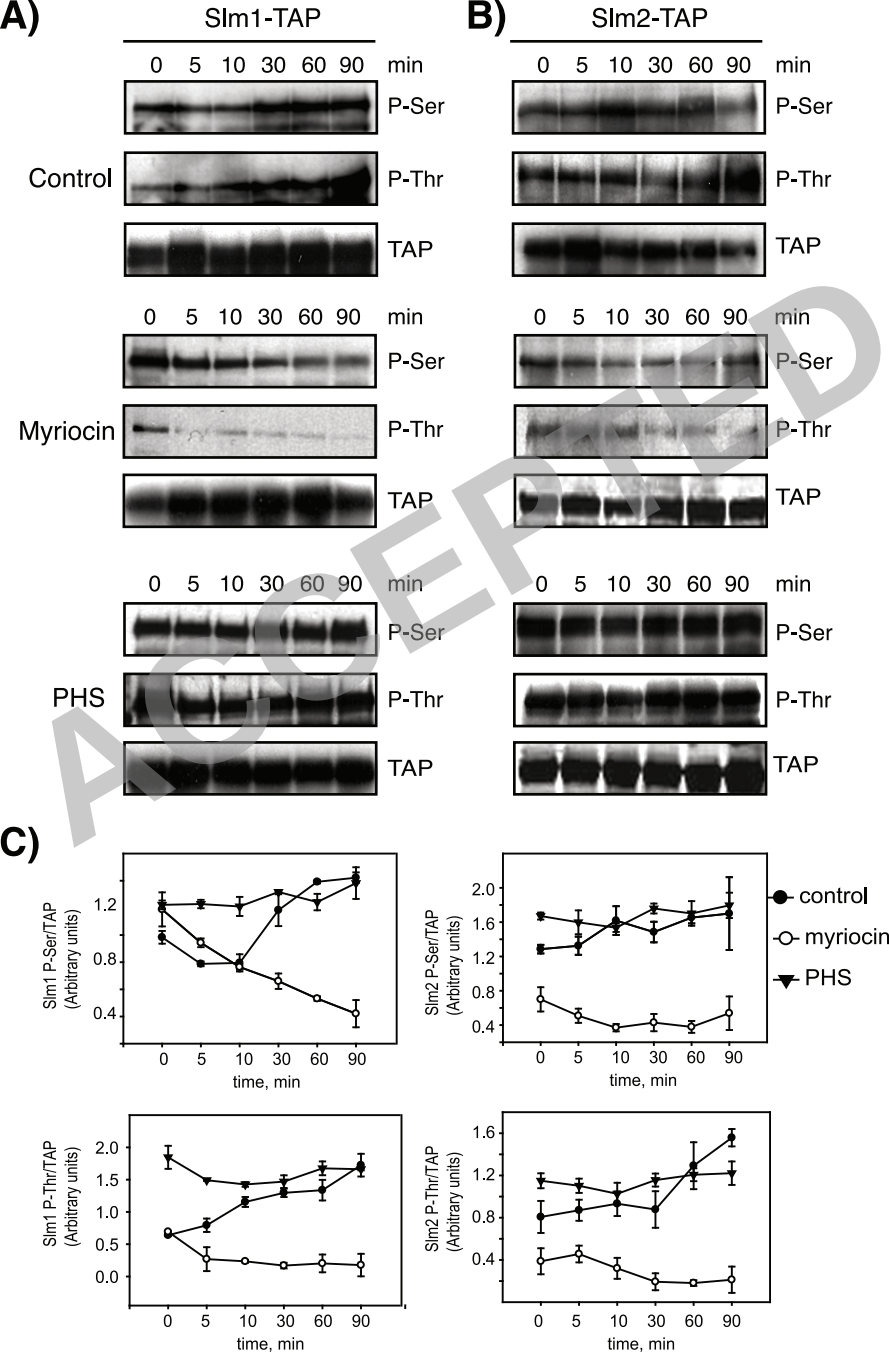
A)
Slm1-TAP
B)
Slm2-TAP
0 5 10 30 60 90 min
P-Ser
P-Thr
TAP
Control
Myriocin
PHS
C)
Slm1 P-Ser/TAP (Arbitrary units)
Slm2 P-Ser/TAP (Arbitrary units)
Slm1 P-Thr/TAP (Arbitrary units)
Slm2 P-Thr/TAP (Arbitrary units)
time, min
control
myriocin
PHS

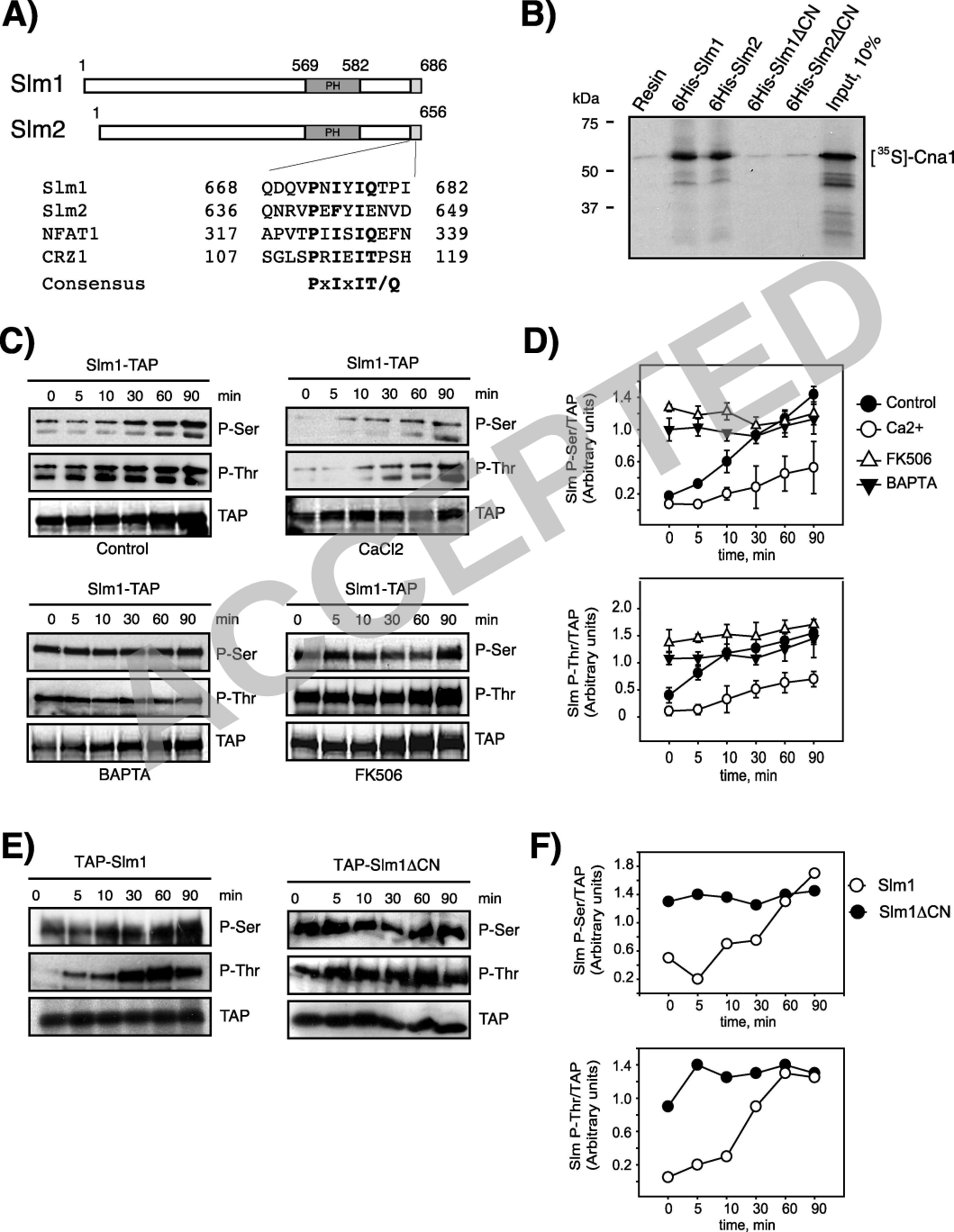
A)
Slm1
1
569
582
686
PH
Slm2
1
656
PH
Slm1 668 QDQVPNIYIQTPI 682
Slm2 636 QNRVPEFYIENVD 649
NFAT1 317 APVTPIISIQEFN 339
CRZ1 107 SGLSPRIEITPSH 119
Consensus PxIxIT/Q
B)
kDa
75
50
37
Resin
6His-Slm1
6His-Slm2
6His-Slm1ΔCN
6His-Slm2ΔCN
Input, 10%
[35S]-Cna1
C)
Slm1-TAP
0 5 10 30 60 90 min
P-Ser
P-Thr
TAP
Control
CaCl2
BAPTA
FK506
D)
Slm P-Ser/TAP (Arbitrary units)
Slm P-Thr/TAP (Arbitrary units)
time, min
Control
Ca2+
FK506
BAPTA
E)
TAP-Slm1
TAP-Slm1ΔCN
0 5 10 30 60 90 min
P-Ser
P-Thr
TAP
F)
Slm P-Ser/TAP (Arbitrary units)
Slm P-Thr/TAP (Arbitrary units)
time, min
Slm1
Slm1ΔCN

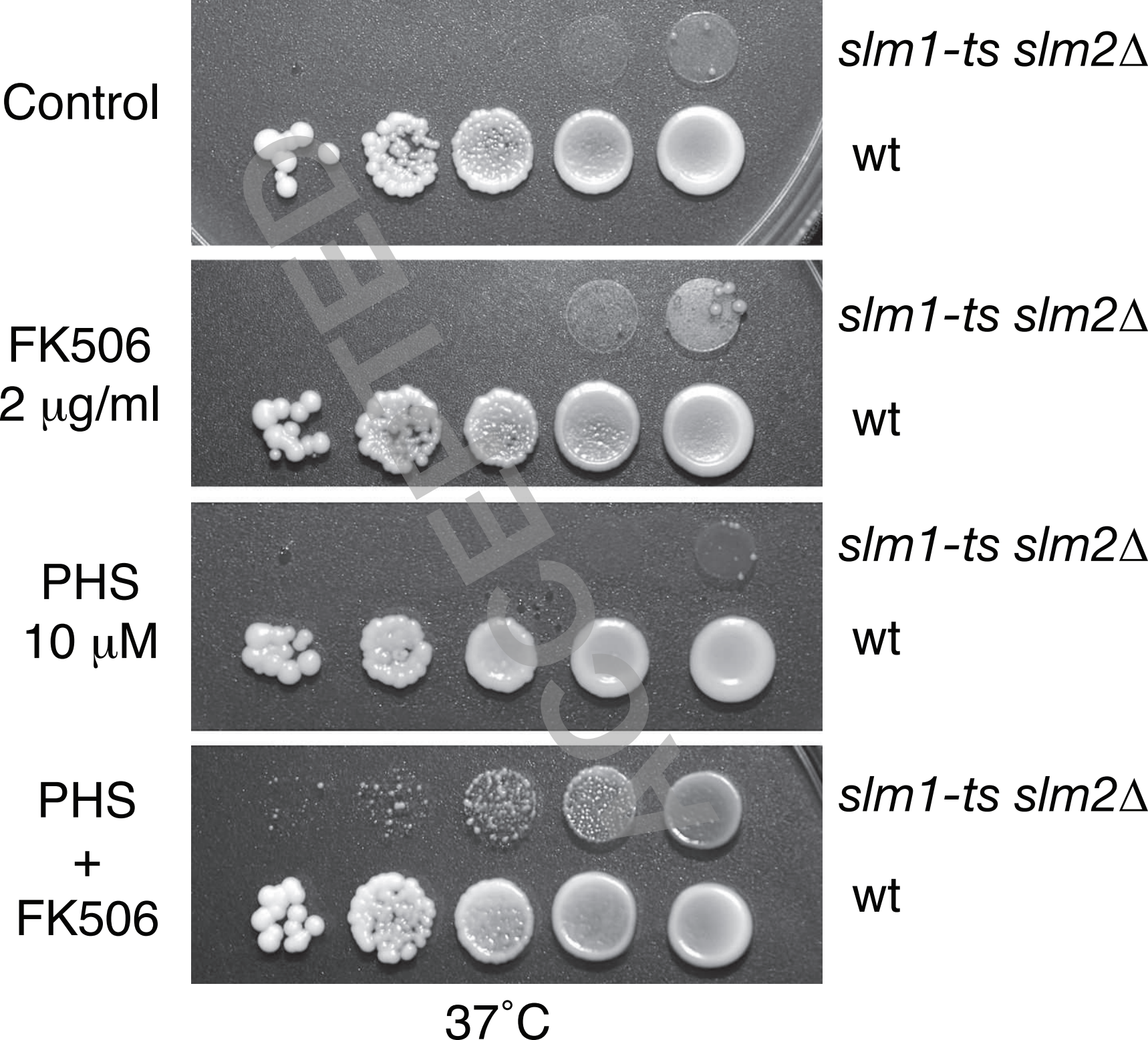
Control
slm1-ts slm2Δ
wt
FK506
2 μg/ml
slm1-ts slm2Δ
wt
PHS
10 μM
slm1-ts slm2Δ
wt
PHS
+
FK506
slm1-ts slm2Δ
wt
37˚C

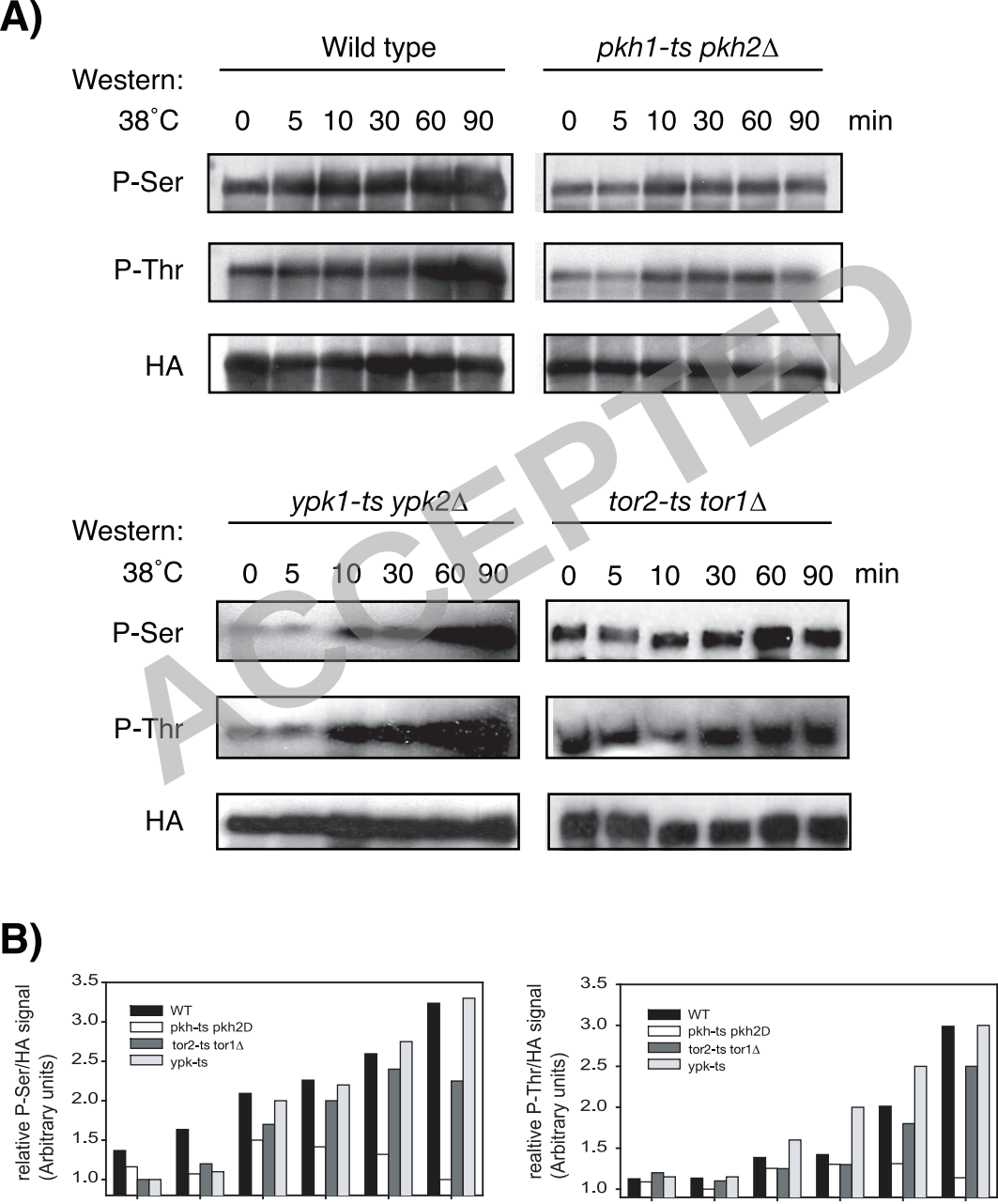
A)
Wild type
pkh1-ts pkh2Δ
Western:
38˚C
0 5 10 30 60 90
0 5 10 30 60 90 min
P-Ser
P-Thr
HA
ypk1-ts ypk2Δ
tor2-ts tor1Δ
Western:
38˚C
0 5 10 30 60 90
0 5 10 30 60 90 min
P-Ser
P-Thr
HA
B)
relative P-Ser/HA signal (Arbitrary units)
WT
pkh-ts pkh2D
tor2-ts tor1Δ
ypk-ts
time, min
realtive P-Thr/HA signal (Arbitrary units)
WT
pkh-ts pkh2D
tor2-ts tor1Δ
ypk-ts
time, min

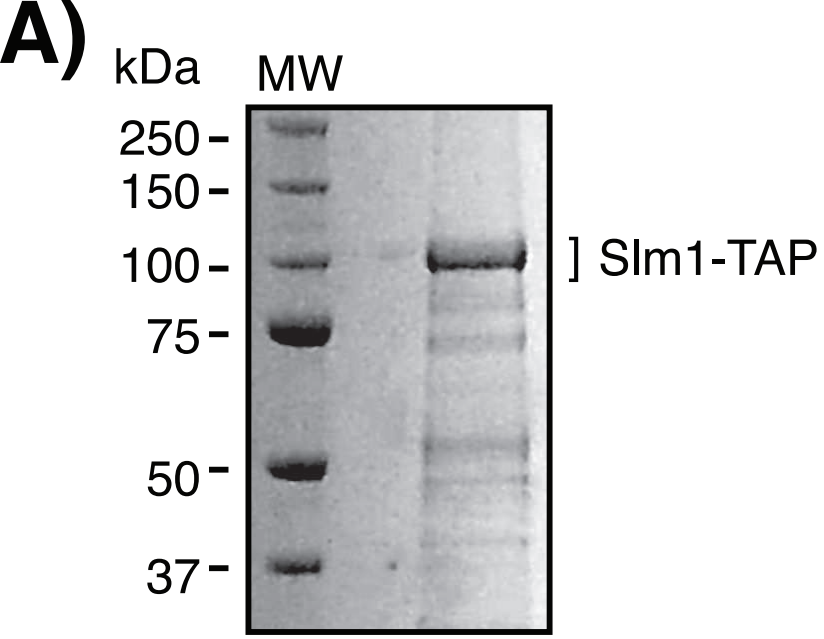
A)
kDa
MW
250
150
100
75
50
37
] Slm1-TAP

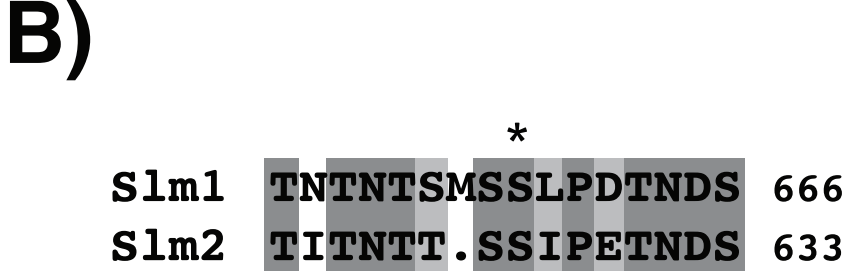
B)
*
Slm1 TNTNTSMSSLPDTNDS 666
Slm2 TITNTT.SSIPETNDS 633

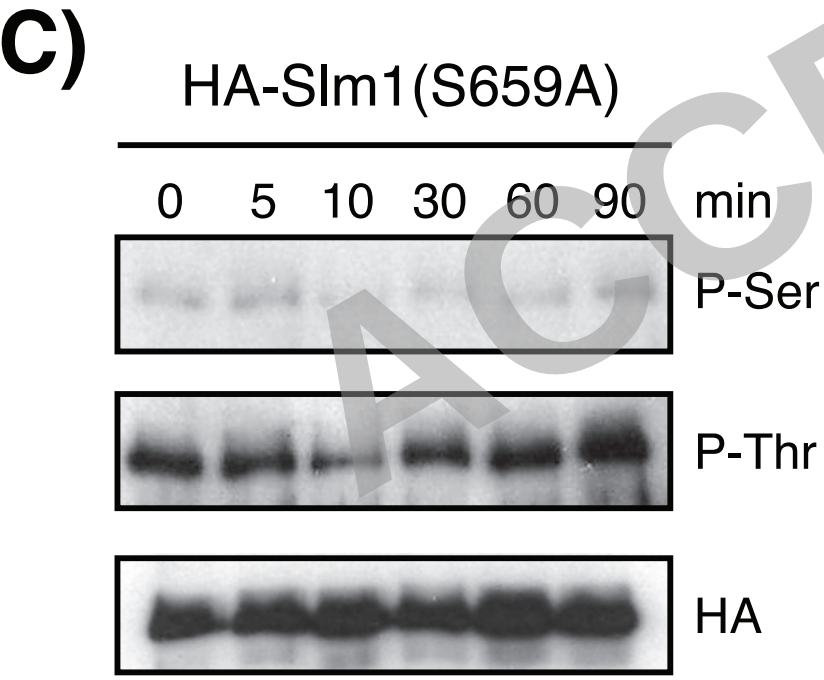
C)
HA-Slm1(S659A)
0 5 10 30 60 90 min
P-Ser
P-Thr
HA

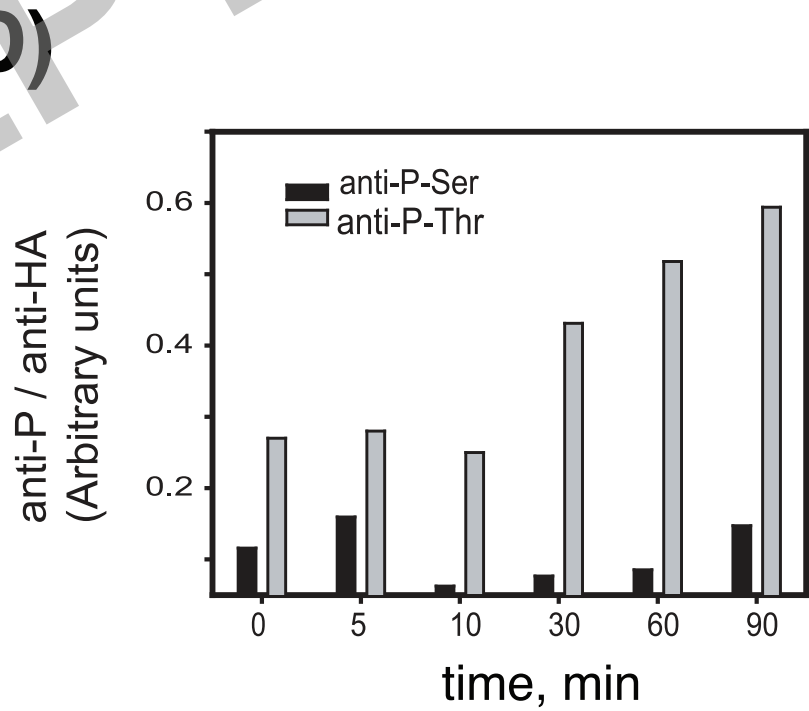
D)
anti-P-Ser
anti-P-Thr
anti-P / anti-HA
(Arbitrary units)
0.6
0.4
0.2
0
5
10
30
60
90
time, min

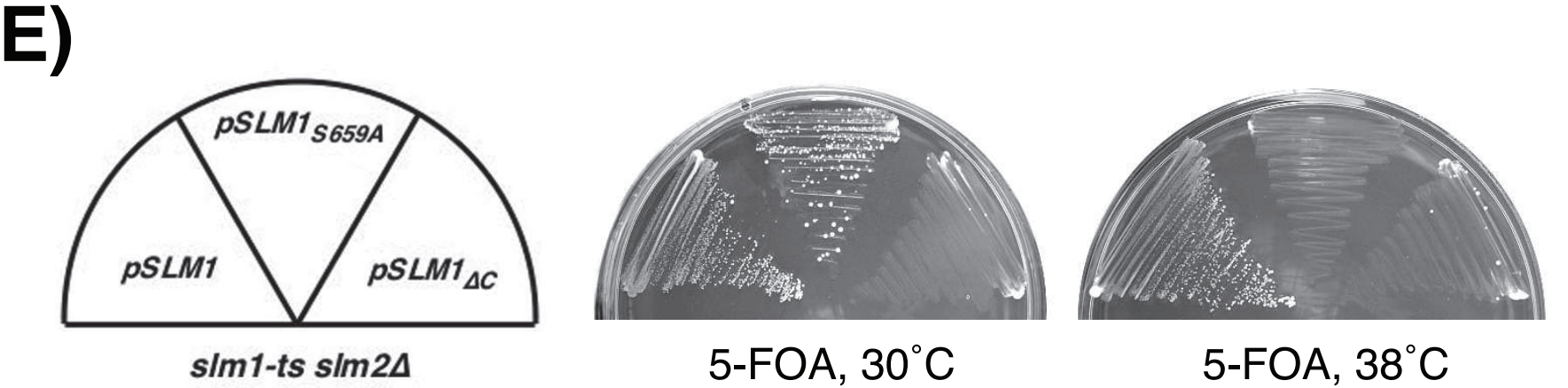
E)
pSLM1 S659A
pSLM1
pSLM1 ΔC
slm1-ts slm2Δ
5-FOA, 30˚C
5-FOA, 38˚C

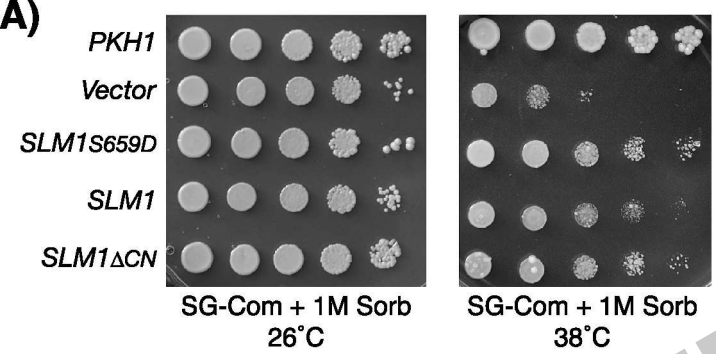
A)
PKH1
Vector
SLM1S659D
SLM1
SLM1ΔCN
SG-Com + 1M Sorb
26˚C
SG-Com + 1M Sorb
38˚C

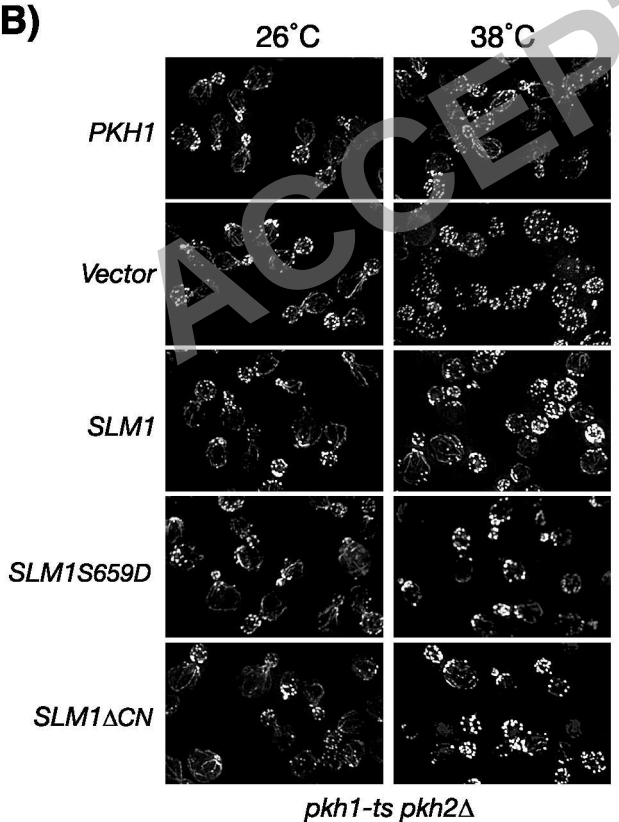
B)
26˚C
38˚C
PKH1
Vector
SLM1
SLM1S659D
SLM1ΔCN
pkh1-ts pkh2Δ

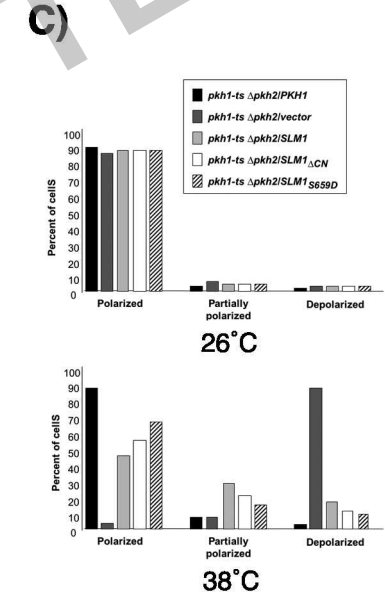
C)
pkh1-ts Δpkh2/PKH1
pkh1-ts Δpkh2/vector
pkh1-ts Δpkh2/SLM1
pkh1-ts Δpkh2/SLM1ΔCN
pkh1-ts Δpkh2/SLM1S659D
Percent of cells
Polarized
Partially polarized
Depolarized
26˚C
38˚C

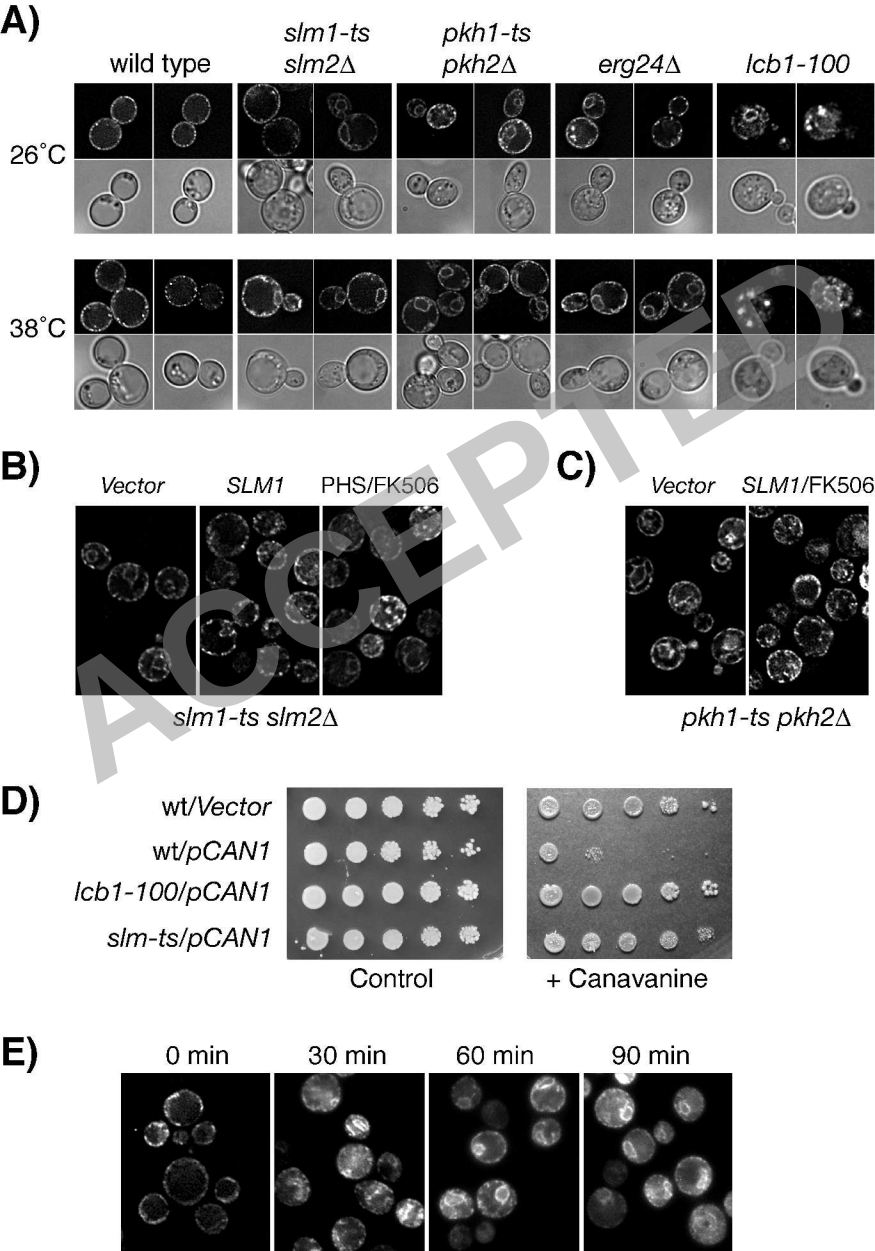
A)
wild type
slm1-ts slm2Δ
pkh1-ts pkh2Δ
erg24Δ
lcb1-100
26˚C
38˚C
B)
Vector
SLM1
PHS/FK506
slm1-ts slm2Δ
C)
Vector
SLM1/FK506
pkh1-ts pkh2Δ
D)
wt/Vector
wt/pCAN1
lcb1-100/pCAN1
slm-ts/pCAN1
Control
+ Canavanine
E)
0 min
30 min
60 min
90 min